

# NAVAL POSTGRADUATE SCHOOL

Monterey, California



## THESIS

### OPTIMALITY OF AEROASSISTED ORBITAL PLANE CHANGES

by

Michael S. Parish II

December 1995

Thesis Advisor:

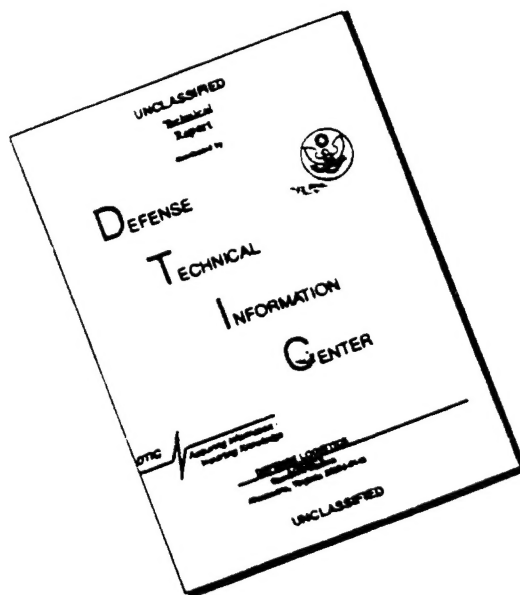
I. Michael Ross

Approved for public release; distribution is unlimited.

19960411 113

DTIC QUALITY INSPECTED 1

# DISCLAIMER NOTICE



THIS DOCUMENT IS BEST QUALITY AVAILABLE. THE COPY FURNISHED TO DTIC CONTAINED A SIGNIFICANT NUMBER OF PAGES WHICH DO NOT REPRODUCE LEGIBLY.

**REPORT DOCUMENTATION PAGE**

Form Approved OMB No. 0704-0188

Public reporting burden for this collection of information is estimated to average 1 hour per response, including the time for reviewing instruction, searching existing data sources, gathering and maintaining the data needed, and completing and reviewing the collection of information. Send comments regarding this burden estimate or any other aspect of this collection of information, including suggestions for reducing this burden, to Washington Headquarters Services, Directorate for Information Operations and Reports, 1215 Jefferson Davis Highway, Suite 1204, Arlington, VA 22202-4302, and to the Office of Management and Budget, Paperwork Reduction Project (0704-0188) Washington DC 20503.

1. AGENCY USE ONLY (Leave blank)	2. REPORT DATE December 1995	3. REPORT TYPE AND DATES COVERED Master's Thesis	
4. TITLE AND SUBTITLE OPTIMALITY OF AEROASSISTED ORBITAL PLANE CHANGES		5. FUNDING NUMBERS	
6. AUTHOR(S) Parish, Michael S.			
7. PERFORMING ORGANIZATION NAME(S) AND ADDRESS(ES) Naval Postgraduate School Monterey CA 93943-5000		8. PERFORMING ORGANIZATION REPORT NUMBER	
9. SPONSORING/MONITORING AGENCY NAME(S) AND ADDRESS(ES) Space Warfare Center, Falcon AFB, Co		10. SPONSORING/MONITORING AGENCY REPORT NUMBER	
11. SUPPLEMENTARY NOTES The views expressed in this thesis are those of the author and do not reflect the official policy or position of the Department of Defense or the U. S. Government.			
12a. DISTRIBUTION/AVAILABILITY STATEMENT Approved for public release; distribution is unlimited.		12b. DISTRIBUTION CODE	
13. ABSTRACT (maximum 200 words)  Future spacecraft designs, and in particular military spacecraft, may incorporate the use of synergetic orbital plane change maneuvers. The analysis of these maneuvers and their optimality is an area in which much work has been done but only a few questions have been answered. This thesis discusses the theoretical background for solving the optimal control problem. A framework is set forth for the formulation of the overall problem which must be solved. Pontryagin's Maximum Principle is applied to obtain the necessary conditions for maximizing the inclination change for a given amount of propellant. Effects of a heating rate constraint imposed by the thermal protection system are considered. The Program to Optimize Simulated Trajectories (POST) is used to obtain results for the Maneuverable Reentry Research Vehicle (MRRV) to illustrate certain points. Two characterizations of the atmospheric pass are analyzed and compared to previous work, namely Aerobang and Aerocruise. A discussion on the limited use of POST as a direct method of analysis is also included.			
14. SUBJECT TERMS Optimal, Trajectory, MRRV, Aeroassisted, Orbital Transfer, Aerobang, Aerocruise, Maximum Principle, Plane Change.		15. NUMBER OF PAGES 111	
		16. PRICE CODE	
17. SECURITY CLASSIFICATION OF REPORT Unclassified	18. SECURITY CLASSIFICATION OF THIS PAGE Unclassified	19. SECURITY CLASSIFICATION OF ABSTRACT Unclassified	20. LIMITATION OF ABSTRACT UL

NSN 7540-01-280-5500

Standard Form 298 (Rev. 2-89)  
Prescribed by ANSI Std. Z39-18 298-102





Approved for public release; distribution is unlimited.

## OPTIMALITY OF AEROASSISTED ORBITAL PLANE CHANGES

Michael S. Parish II

Lieutenant, United States Navy

B. S. M. A., United States Naval Academy, 1988

Submitted in partial fulfillment of the  
requirements for the degree of

## MASTER OF SCIENCE IN ASTRONAUTICAL ENGINEERING

from the

## NAVAL POSTGRADUATE SCHOOL

December 1995

Author:

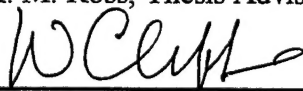


Michael S. Parish II

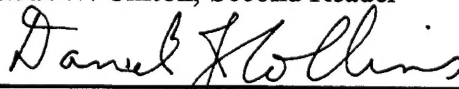
Approved by:



I. M. Ross, Thesis Advisor



LCDR W. Clifton, Second Reader



Daniel J. Collins, Chairman

Department of Aeronautical and Astronautical Engineering



## ABSTRACT

Future spacecraft designs, and in particular military spacecraft, may incorporate the use of synergetic orbital plane change maneuvers. The analysis of these maneuvers and their optimality is an area in which much work has been done but only a few questions have been answered. This thesis discusses the theoretical background for solving the optimal control problem. A framework is set forth for the formulation of the overall problem which must be solved. Pontryagin's Maximum Principle is applied to obtain the necessary conditions for maximizing the inclination change for a given amount of propellant. Effects of a heating rate constraint imposed by the thermal protection system are considered. The Program to Optimize Simulated Trajectories (POST) is used to obtain results for the Maneuverable Reentry Research Vehicle (MRRV) to illustrate certain points. Two characterizations of the atmospheric pass are analyzed and compared to previous work, namely Aerobang and Aerocruise. A discussion on the limited use of POST as a direct method of analysis is also included.



## TABLE OF CONTENTS

I.	INTRODUCTION.....	1
II.	PROBLEM STATEMENT AND MODELING.....	5
	A. THE PROBLEM .....	5
	B. EXOATMOSPHERIC PORTION.....	6
	C. COORDINATE SYSTEM AND EQUATIONS OF MOTION.....	6
	D. THE PLANET MODEL.....	9
	E. THE VEHICLE MODEL.....	9
III.	THEORETICAL ANALYSIS (INDIRECT METHOD).....	15
	A. GENERAL PROBLEM FORMULATION .....	15
	B. THE BASIC MAXIMUM PRINCIPLE.....	16
	C. THE RESTRICTED MAXIMUM PRINCIPLE. ....	17
	D. JUMP CONDITIONS .....	19
	E. THE COMPLETE FORMULATION.....	20
	F. APPLICATION OF THE RESTRICTED MAXIMUM PRINCIPLE ....	21
IV.	NUMERICAL ANALYSIS (DIRECT METHOD) .....	33
	A. POST.....	33
	B. TRAJECTORY CHARACTERIZATION.....	34
	C. THE MAN IN THE LOOP.....	39
	D. TRAJECTORY RESULTS.....	41
V.	CONCLUSIONS AND RECOMMENDATIONS.....	55
	A. CONCLUSIONS.....	55
	B. RECOMMENDATIONS FOR FURTHER STUDY.....	56
	APPENDIX A. SAMPLE POST INPUT FILE (AEROBANG).....	57
	APPENDIX B. SAMPLE POST INPUT FILE (AEROCUISE).....	71
	APPENDIX C. MAPLE PROGRAM OUTPUT.....	83
	LIST OF REFERENCES.....	93
	INITIAL DISTRIBUTION LIST.....	95



## LIST OF SYMBOLS

$b_i$	control constraint functions
$B$	set of allowable states
$C$	constant of proportionality in Chapman's equation
$C_A$	axial force coefficient for MRRV
$C_{A_{PR}}$	pressure term of axial force coefficient for MRRV
$C_{A_{SF}}$	skin friction term of axial force coefficient for MRRV
$C_D(\alpha)$	drag coefficient as a function of $\alpha$
$C_L(\alpha)$	lift coefficient as a function of $\alpha$
$C_N$	normal force coefficient for MRRV
$D(\alpha)$	magnitude of the atmospheric drag as a function of $\alpha$
$f$	state derivative vector function
$f_0$	integral portion of performance index
$F$	target vector function
$g$	acceleration of gravity
$g_0$	acceleration of gravity at sea level
$G$	state constraint function
$h$	altitude
$H$	Hamiltonian function
$i$	orbital inclination
$i_{deorbit}$	inclination change due to deorbit impulse
$I_{sp}$	rocket motor specific impulse in seconds
$J$	performance index
$k$	number of control constraint functions
$L$	Lagrangian function
$L(\alpha)$	magnitude of the atmospheric lift as a function of $\alpha$
$(L/D)_{max}$	maximum lift to drag ratio

$m$	vehicle mass
$m$	number of target functions
$m_{exit}$	mass of vehicle upon atmospheric exit
$M$	maximum function
$n$	number of states
$p$	state constraint boundary function
$\dot{q}$	vehicle stagnation point heating rate
$r$	radial distance from center of central body
$r_0$	local reference radius for atmospheric density
$R_{atm}$	radius of the atmospheric entry
$R_{exit}$	vehicle radius on atmospheric exit
$R_{orbit}$	radius of the initial circular orbit
$s$	number of controls
$T$	thrust
$\mathbf{u}$	control vector
$\mathbf{u}^*$	optimal control vector
$\mathbf{U}$	set of admissible controls
$v$	vehicle speed
$V_{entry}$	vehicle speed on atmospheric entry
$V_{exit}$	vehicle speed on atmospheric exit
$V_{orbit}$	vehicle speed in initial circular orbit
$\Delta V_{deorbit}$	magnitude of the deorbit Impulse characteristic velocity
$\mathbf{x}$	state vector
$\mathbf{x}^*$	optimal state vector
$\mathbf{x}_0$	initial state vector
$z$	state constraint function exponent



$\alpha$	angle of attack,
$\beta$	local exponential scale factor for the atmospheric density
$\gamma$	flight path angle
$\gamma_{entry}$	flight path angle on atmospheric entry
$\gamma_{exit}$	flight path angle on atmospheric exit
$\delta$	angle of bank
$\nabla_x$	gradient taken with respect to the vector $\mathbf{x}$
$\phi$	vehicle latitude
$\Phi$	terminal payoff portion of performance index
$\eta$	Lagrange multiplier for state constraint
$\kappa_i$	Lagrange multiplier for control constraints
$\lambda$	costate vector
$\lambda_r$	costate for radius
$\lambda_v$	costate for speed
$\lambda_\gamma$	costate for flight path angle
$\lambda_\phi$	costate for latitude
$\lambda_\psi$	costate for heading angle
$\lambda_m$	costate for mass
$\lambda^*$	optimal costate vector
$\mu$	earth's gravitational constant
$\rho$	atmospheric density
$\rho_0$	atmospheric density at radius $r_0$
$\sigma$	side-slip or yaw angle
$\sigma_{deorbit}$	side slip angle of the vehicle or retro-rocket used for the deorbit impulse
$\tau$	scaling dependent time variable
$\theta$	vehicle longitude
$\psi$	vehicle heading angle
$\xi$	as defined in Equation (68)

## ACKNOWLEDGMENTS

The author would like to acknowledge the financial support of Space Warfare Center , Falcon AFB, for allowing the purchase of equipment and travel in support of this thesis.

The author wants to thank Prof. I. M. Ross for his guidance and patience during the work on this thesis.

The author would like to thank his wife Angela and children for their loving support during the long hours of required for the completion of this work.

The author would like to thank most of all the Lord God Almighty for the gifts and talents needed to complete this work.

## I. INTRODUCTION

Aeroassisted orbital plane changes offer the potential of significant fuel savings over purely exoatmospheric propulsive maneuvers. Some of the possible applications for this maneuver are:

- (1) an evasive maneuver for a satellite being pursued by an enemy ASAT,
- (2) an ASAT constellation containing many ASAT's parked in some benign looking orbit that maneuver when needed into the orbit of a target satellite,
- (3) for an intelligence satellite to gather intelligence at a very low altitude or to visit a specified location faster than an exoatmospheric satellite,
- (4) for a reusable ferry between a repair station and a damaged satellite at different inclinations,
- (5) for a repair satellite to perform repairs local to a damaged satellite while being stationed at a repair station.

Some of these orbital transfer applications may require large plane changes to be made in a single pass. Much work has been done in the area of analyzing possible trajectories for this type of maneuver. Three distinct trajectories are discussed in the literature as potential optimal solutions. These are Aeroglide, Aerocruise, and Aerobang. All of these maneuvers involve a deorbit impulse, an aerodynamic turn in the atmosphere, a reorbit impulse and a circularization impulse. The difference between the maneuvers is in the aerodynamic turn. [Refs. 1-6]

For Aeroglide, the vehicle performs the plane change solely with the lift generated by the vehicle surfaces. A portion of the lift generated is normal to the orbit plane and the angle of attack is usually close to  $(L/D)_{max}$ . In order to generate the necessary lift, the vehicle is flown at high velocities and low altitudes where the atmosphere is dense resulting in, sometimes, excessively high heating rates. Aeroglide is an unconstrained maneuver in terms of heating rate, meaning that no heating rate limit is taken into account. The only fuel expenditures are in the deorbit, reorbit and circularization impulses which has been shown to be significantly less than the purely propulsive exoatmospheric case [Ref. 7]. The tradeoff between Thermal Protection System (TPS) mass and fuel consumption is a design area which restricts the amount of

plane change which can be achieved by an Aeroglide maneuver. When a maneuver is required to achieve a larger plane change than is possible with the unconstrained Aeroglide, propulsive power must be used to control the heat rate during the turn. Aerocruise and Aerobang are two schemes for doing just that.

The aerodynamic turn in both Aerocruise and Aerobang consists of a zero thrust arc from atmosphere entry until the maximum heating rate is reached and a propulsive arc at constant heating rate followed by a zero thrust arc to atmosphere exit. The difference between the two maneuvers is in the characteristics of the heat rate control arc.

Aerocruise uses a throttled thrust to cancel drag and a component of lift to maintain a constant altitude. This results in a circular arc at constant velocity and altitude maintaining a constant heating rate. Aerobang, on the other hand, uses zero thrust or maximum thrust and modulates the angle of attack and angle bank to vary altitude (and thus density) and speed while maintaining a constant heating rate.

The question then arises, "What is the optimal maneuver to maximize the orbital plane change of a circular orbit for a given amount of propellant?" The answer to this question remains unknown. This thesis will build directly on the work of two previous authors. The first is Thomas P. Spriesterbach who performed a comparison of two vehicles designed for synergetic maneuvers and their performance in all three of the above profiles [Ref. 2]. The two vehicles, one of which will be discussed in more detail later, are the Entry Research Vehicle (ERV) and the Maneuverable Reentry Research Vehicle (MRRV). In his analysis, which considered only at the atmospheric portion of the maneuver, he concluded that the MRRV was superior to the ERV in performance and that the Aerobang maneuver was superior to Aerocruise in terms of plane change in the atmospheric portion of the maneuver. His analysis did not, however, consider the overall maneuver from orbit to orbit. John C. Nicholson, who used the Program to Optimize Simulated Trajectories (POST) to compare the three profiles for the orbit to orbit maneuver using the ERV [Ref. 1], concluded that the Aerobang maneuver was superior in inclination change to Aerocruise. Neither of these works included theoretical justification for the choice of the maneuvers or an overall orbit analysis.

This thesis extends the above works with a major emphasis placed on the theoretical setup of the optimal control problem. It is important to note from the start that this work was done in an attempt to learn about the optimal trajectory for the aeroassisted orbital plane change from a low earth circular orbit to another low earth circular orbit of the same radius. As will be seen, even this apparently narrow problem can be very complex. Although later there will be numerical analysis of two particular feasible trajectories no claim is being made here as to the optimality of any particular trajectory. However, there is theoretical data available which narrows the search when looking for the optimal trajectory. It is difficult to solve the resulting two point boundary value problem (TPBVP) due to the typical small radius of convergence; however, much can be learned from the theory which can aid in the direct methods to numerically solve this problem. A discussion is also included on how to extend this thesis to obtain the needed knowledge of the costate values and allow a solution to the TPBVP. This thesis develops the set of necessary conditions for the optimal trajectory and discusses a method for handling the small radius of convergence.



## II. PROBLEM STATEMENT AND MODELING

For the purpose of this thesis the term optimal will be used in the sense of the largest inclination change for a given amount of fuel expended during the maneuver from the initial circular orbit to the final circular orbit. A formulation of the problem is established which is conducive to determining the overall optimal solution.

### A. THE PROBLEM

The overall optimization problem for the orbital plane change is an optimization problem attempting to achieve the maximum orbital plane change using the available fuel. The total fuel to carry out the maneuver consists of the sum of the propellant used for the deorbit impulse, the atmospheric pass and the reorbit and circularization impulses. This allows many possibilities of how to analyze the problem. Since the exoatmospheric impulses are discrete in nature they could be thought of as discrete parameters. They can also be used to contribute to the total inclination change if not fired completely in the plane of the current orbit. It has been shown by Miele and Lee [Ref. 5] that by applying the exoatmospheric impulses slightly out of plane, improvements in performance can be achieved. The out of plane yaw angles used for each impulse would then become additional parameters of the optimization problem. This overall problem could be treated as a parameter optimization problem attempting to maximize the total inclination change during four discrete events, the deorbit impulse, the atmospheric pass and the reorbit and circularization impulses. In this case, it would be necessary to create an algorithm to solve for the optimal control history of an atmospheric pass starting with the initial atmospheric entry conditions dictated by the deorbit impulse and terminating at the atmospheric exit conditions dictated by the reorbit and circularization impulses. The theory which will be considered for the optimization of the atmospheric pass will be discussed in later chapters. The remainder of this chapter will be devoted to the modeling and formulation issues present in the overall problem.

*(Note: All variable definitions are stated in the List of Symbols at the front of this thesis)*

## B. EXOATMOSPHERIC PORTION

The three impulses which are performed outside the atmosphere would determine the entry and exit conditions for the atmospheric optimal control problem. For example, once the  $\sigma_{deorbit}$  and  $\Delta V_{deorbit}$  are chosen, the equations for conserving energy and angular momentum will determine the entry velocity and flight path angle. In like manner, once the  $\Delta V_{reorbit}$ ,  $\Delta V_{circ}$  and their associated  $\sigma$ 's are chosen, the atmospheric  $V_{exit}$  and  $\gamma_{exit}$  will be fixed. The inclination change from  $\Delta V_{reorbit}$  can be found looking at the vector velocities as:

$$i_{deorbit} = \tan^{-1} \left( \frac{\Delta V_{deorbit} \sin(\sigma_{deorbit})}{V_{orbit} - \Delta V_{deorbit} \cos(\sigma_{deorbit})} \right) \quad (1)$$

The other inclination changes associated with the impulses can be found in like manner.

Other known entry and exit boundary conditions are the entry and exit radii which are both equal to  $R_{atm}$ . The entry  $\theta$ ,  $\phi$  and  $\psi$  angles are also fixed from the Keplerian elliptical deorbit at the radius  $R_{atm}$ . Also the entry and exit masses will be fixed by the fuel expended during the impulses. Thus, the entire entry state vector is fixed by choosing  $R_{atm}$ ,  $\sigma_{deorbit}$  and  $\Delta V_{deorbit}$ . Also, a target state space is set since  $m_{exit}$ ,  $V_{exit}$ ,  $\gamma_{exit}$  and  $R_{exit}$  are specified by the exoatmospheric parameters. This leaves three exit states free for the algorithm to use in the optimization process.

## C. COORDINATE SYSTEM AND EQUATIONS OF MOTION

The coordinate system and equations of motion used here are for a lifting body in an inverse square gravity field. These equations are derived by Vinh [Ref. 14], and assume a spherical central body and a non-rotating atmosphere. The vehicle is a point mass experiencing aerodynamic forces.

The state vector is:

$$[r \ v \ \gamma \ \theta \ \phi \ \psi \ m]^T$$

The control vector is:

$$[\alpha \ \delta \ \sigma \ T]^T$$



The gravitational field is :

This system is depicted in Figure 1 below.


$$\frac{dr}{dt} = v \sin(\gamma) \quad (3)$$

7

$$\frac{v}{dt} \frac{d\gamma}{dt} = \frac{(L(\alpha) + T \sin(\alpha)) \cos(\delta)}{m} - \frac{\mu \cos(\gamma)}{r^2} + \frac{v^2 \cos(\gamma)}{r} \quad (5)$$

$$\frac{d\theta}{dt} = \frac{v \cos(\gamma) \cos(\psi)}{r \cos(\phi)} \quad (6)$$

$$\frac{d\phi}{dt} = \frac{v \cos(\gamma) \sin(\psi)}{r} \quad (7)$$

$$\frac{v}{dt} \frac{d\psi}{dt} = \frac{(L(\alpha) + T \sin(\alpha)) \sin(\delta)}{m \cos(\gamma)} - \frac{v^2 \cos(\gamma) \cos(\psi) \tan(\phi)}{r} \quad (8)$$

$L(\alpha)$  and  $D(\alpha)$  are computed as:

$$D(\alpha) = \frac{1}{2} \rho v^2 A C_D(\alpha) \quad (9)$$

$$L(\alpha) = \frac{1}{2} \rho v^2 A C_L(\alpha) \quad (10)$$

From the rocket equation we have the mass state derivative:

$$\frac{dm}{dt} = - \frac{T}{I_{sp} g_0} \quad (11)$$

The orbital inclination at any time is given by:

$$\cos(i) = \cos(\phi) \cos(\psi) \quad (12)$$

The heat rate is determined by using Chapman's equation:

$$\frac{dq}{dt} = C \rho^{0.5} v^{3.15} \quad (13)$$

The heating rate used in this thesis will be:  $100 \frac{\text{Btu}}{\text{ft}^2 - \text{sec}}$  or  $1.13 \times 10^6 \frac{\text{W}}{\text{m}^2}$ . This specific value was used here for comparisons to be made later.

Density is modeled as locally exponential for analytical purposes, that is:

$$\rho = \rho_0 e^{-\beta(r-r_0)} \quad (14)$$

#### D. THE PLANET MODEL

The planet model used throughout this section is a spherical earth with a non-rotating locally exponential atmosphere. The 1962 U.S. standard atmosphere is used in the numerical analysis with the local  $\beta$  derived from that data.

#### E. THE VEHICLE MODEL

The vehicle used throughout this thesis is the MRRV which has the following characteristics. [Refs. 2,4]

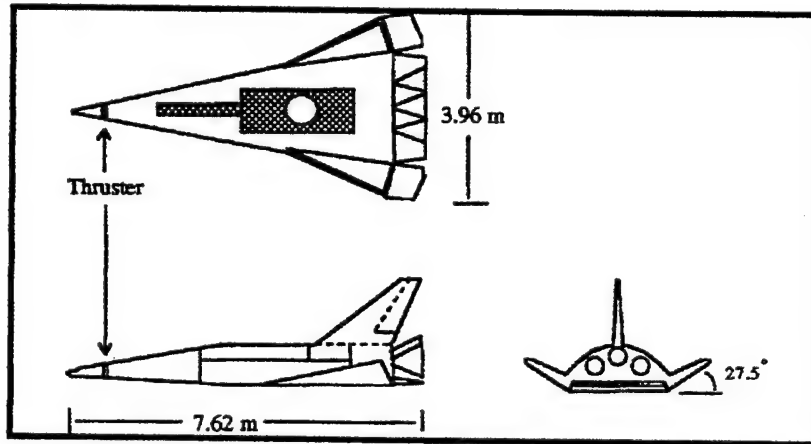


Figure 2: MRRV Diagram from [Ref. 2]

**Mass (fully fueled):** 4899 kg

**Fuel capacity:** 2615 kg

**Aerodynamic reference area:**  $11.7 \text{ m}^2$

**Engine characteristics and Isp:** Three Marquardt R-40-B rocket motors make up the propulsion system, providing a total of 14679 N of thrust at a specific impulse of 300 sec.

### Aerodynamic Coefficients:

The aerodynamic data for the MRRV comes from an analytic computer extrapolation of wind tunnel data taken by the Air Force Flight Dynamics Laboratory (AFFDL). The actual wind tunnel tests were performed on a scale model of the MRRV at transonic Mach numbers as well as Mach 3 and Mach 5 [Ref. 8]. This original data is available in tabular form either from AFFDL or the Naval Postgraduate School library. This data was then adjusted to take into account the increase in Mach number and altitude experienced in the orbital maneuver environment. The analytic projections are tabulated in terms of polynomial fits for axial and normal force coefficients in [Ref. 4]. Although this data is given for various Mach numbers the only data used in this thesis is that for Mach 20+ since the entire maneuver takes place in that range. A typographical error was noted in [Ref. 4] in the exponent of one of the polynomial coefficients. The corrected fit data is listed below. The axial force coefficient is composed of a skin friction term and a pressure term that is,

$$C_A = C_{A_{SF}} + C_{A_{PR}} \quad (15)$$

where

$$C_{A_{SF}} = A_1 h^2 + B_1 h + C_1 \quad (16)$$

$h = 210000$  ft was used as a representative altitude, giving a value of .0105 for the skin friction term.

$$C_{A_{PR}} = A_2 \alpha^2 + B_2 \alpha + C_2 \quad (17)$$

$$C_N = A_3 \alpha^2 + B_3 \alpha + C_3 \quad (18)$$

$\alpha$  in degrees,  $0^\circ \leq \alpha \leq 40^\circ$ .

The values used here are given below:

subscript	A	B	C
1	1.38E-12	-3.81E-7	.0297
2 ( $0^\circ \leq \alpha < 16^\circ$ )	1.33E-5	-8.19E-4	.0243
2 ( $16^\circ \leq \alpha < 40^\circ$ )	-6.25E-6	3.58E-4	.0105
3	4.38E-4	6.50E-3	-.035

The one piece of data which was noted as an error in [Ref. 4] was the exponent for  $B_3$ .

The data from these polynomials was then transformed into lift and drag coefficients using the following equations:

$$C_D = C_A \cos(\alpha) + C_N \sin(\alpha) \quad (19)$$

$$C_L = C_N \cos(\alpha) - C_A \sin(\alpha) \quad (20)$$

Once transformed a cubic polynomial was then fit to the lift and drag coefficients, using a least squares fit, yielding the following polynomials:

$$C_D = (4.9852E-6)\alpha^3 + (2.2429E-4)\alpha^2 - (2.4732E-3)\alpha + (3.6994E-2) \quad (21)$$

$$C_L = (-5.8340E-6)\alpha^3 + (5.6214E-4)\alpha^2 + (5.0475E-3)\alpha - (3.3418E-2) \quad (22)$$

For  $\alpha$  in degrees,  $0^\circ \leq \alpha \leq 40^\circ$ .

These are depicted below as well as the lift to drag ratio for use as the aerodynamic model for this thesis. These plots are of the curve fit data, but are indistinguishable from the plotted data on the same scale. The errors in the fit data from the data in [Ref. 4] are shown in Figure 6 through Figure 8. Figure 6 shows the percent error in the lift coefficient fit data for  $\alpha \geq 10$  degrees. The percent errors are larger below 10 degrees because the lift coefficient goes through zero. Therefore, the absolute error is shown for  $\alpha < 10$  degrees in Figure 7. The percent error in the drag coefficients data is shown in Figure 8.

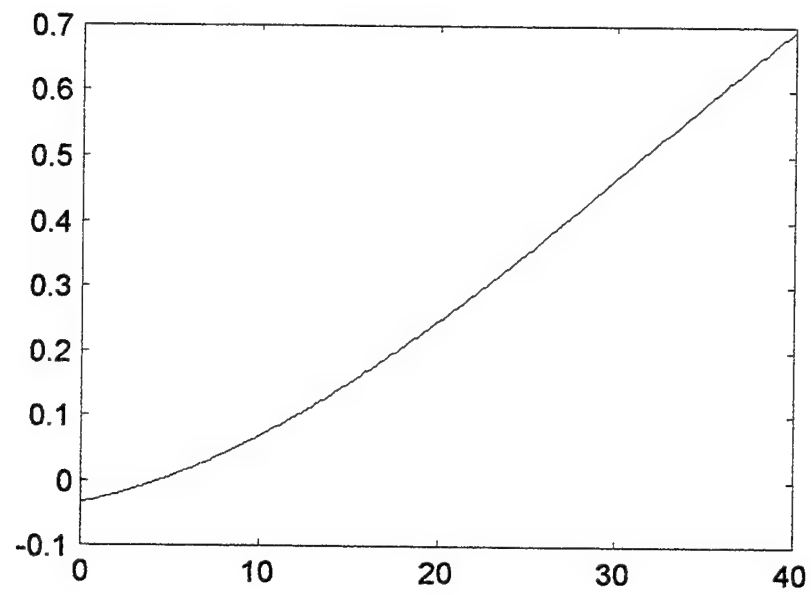


Figure 3: Lift Coefficient vs. Angle of Attack

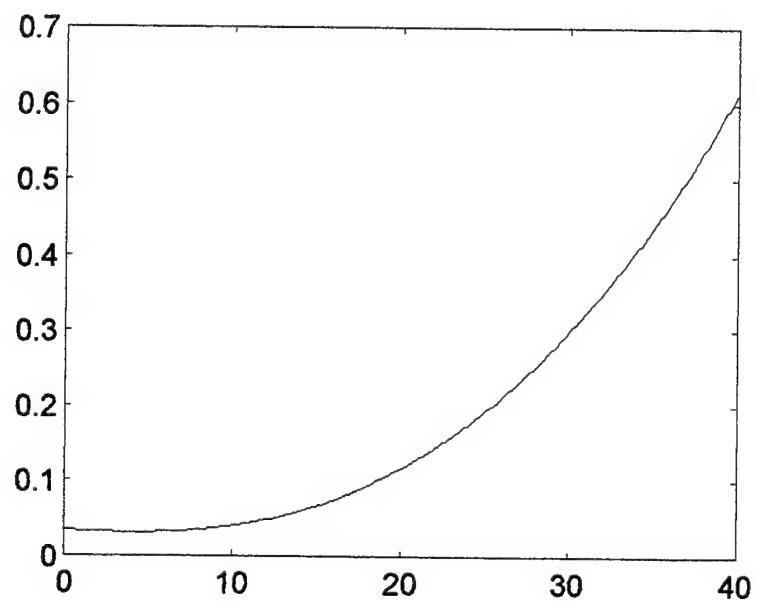


Figure 4: Drag Coefficient vs. Angle of Attack

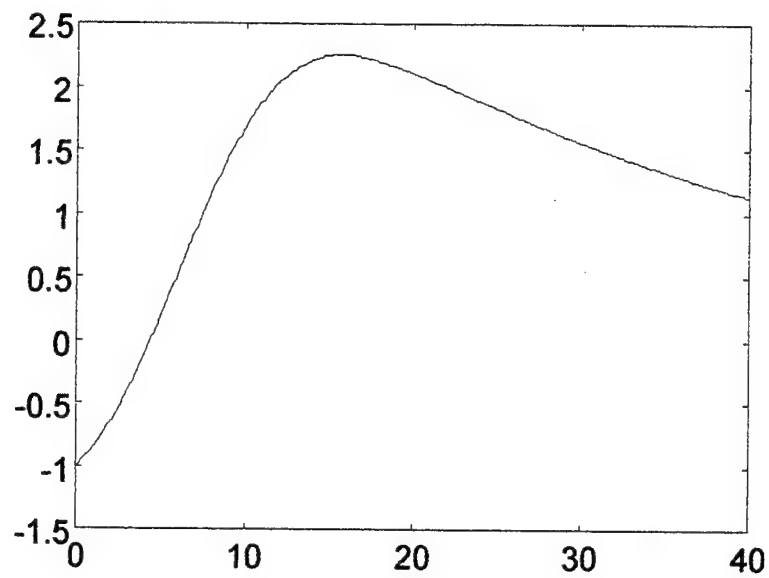


Figure 5: Lift to Drag Ratio vs. Angle of Attack

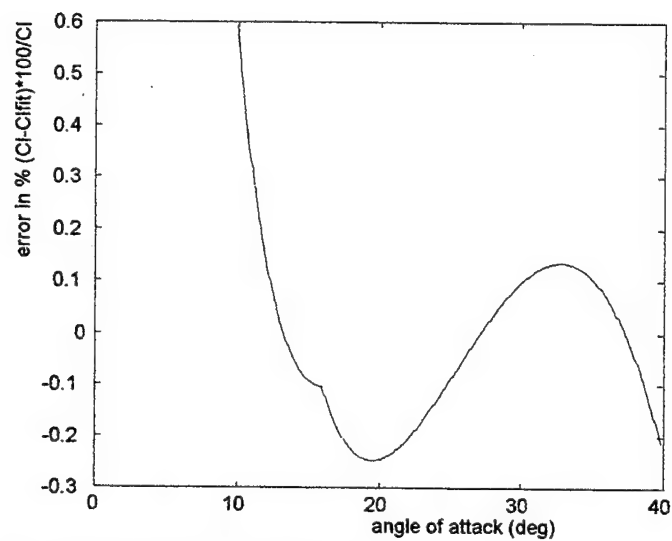


Figure 6: Error in Lift Coefficient (%) vs. Angle of Attack

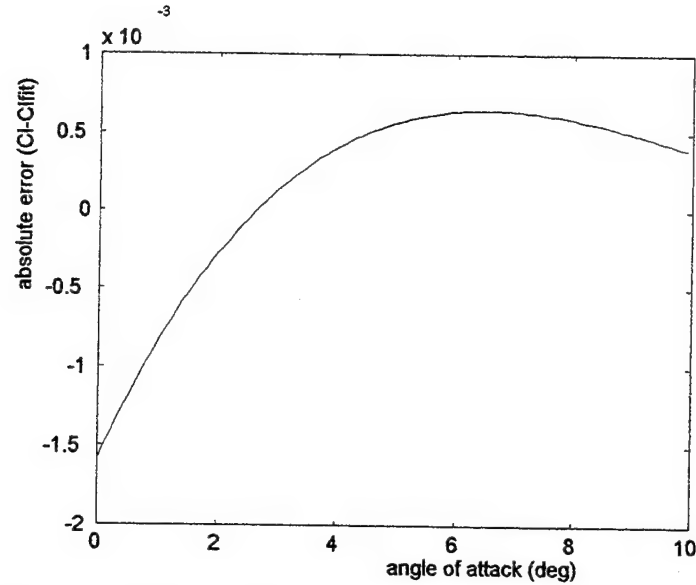


Figure 7: Absolute Error in Lift Coefficient vs. Angle of Attack

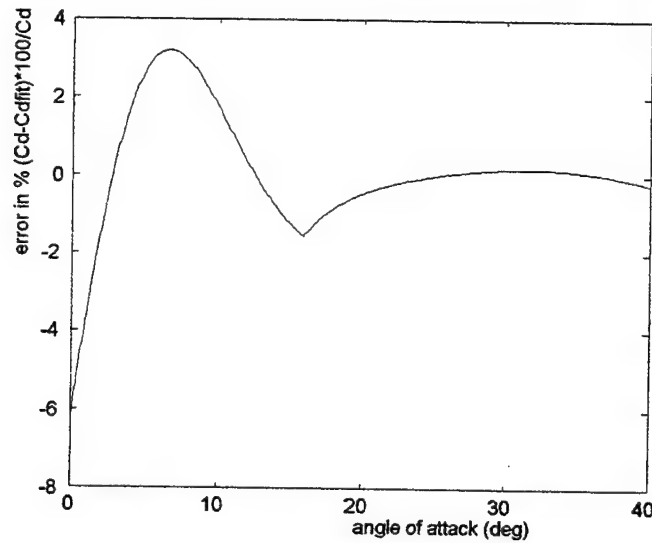


Figure 8: Error in Drag Coefficient (%) vs. Angle of Attack

In order to solve the above problem, many approaches may be taken. There are various “direct methods” and some “indirect methods” of performing this maximization of the final inclination. The next chapter will consider the theory of an indirect approach and the application of the indirect method to solve the above problem. Then some direct method analysis will be considered to explore what is learned through the indirect theory.



### III. THEORETICAL ANALYSIS (INDIRECT METHOD)

The Restricted Maximum Principle refers to that version of the Pontryagin's Maximum Principle (PMP) which incorporates state variable constraints. This material is dealt with in many optimal control texts. However, the notation and the discussion are such that it is necessary to review multiple texts to obtain a good understanding of how to formulate this problem. This chapter will establish the notation and definitions to be used in this thesis with regard to this Restricted Maximum Principle (RMP) which is a combination from various sources. [Refs. 9-11] are the principal texts for this formulation. Also, this discussion is not intended to serve as a general theoretical presentation of the RMP but rather as background for applying the principle to this constrained plane change optimization. The theorems are presented without proof. See the above texts for more detailed discussions.

#### A. GENERAL PROBLEM FORMULATION

Consider the autonomous control problem given:

- a)  $\dot{\mathbf{x}} = \mathbf{f}(\mathbf{x}, \mathbf{u})$ ,  $\mathbf{x} \in \mathbf{R}^n$ ,  $\mathbf{u} \in \mathbf{R}^s$  with  $\mathbf{f}$  continuously differentiable.
- b) the initial point  $\mathbf{x}_0$  and the final target in the form of a vector valued function  $\mathbf{F}(\mathbf{x}(t_f), t_f) \in \mathbf{R}^m$  such that  $\mathbf{F}=0$  implies that the target is hit,
- c) the class of admissible controls, which is taken to be all piecewise continuous functions  $\mathbf{u}$ , with  $\mathbf{u}(t) \in \mathbf{U}$ ,  $\mathbf{U} \subseteq \mathbf{R}^s$
- d) the state constraint which requires  $\mathbf{x}(t)$  to lie in a closed region B of the state space  $\mathbf{R}^n$  of the form

$$B = \{ \mathbf{x} : G(\mathbf{x}) \leq 0 \} \quad (23)$$

for some given scalar-valued function  $G$ , having continuous second partial derivatives, and for which

$$\nabla_{\mathbf{x}} G = \left( \frac{\partial G}{\partial x_1}, \dots, \frac{\partial G}{\partial x_n} \right) \quad (24)$$

does not vanish on the boundary of B, that is, on  $\{ \mathbf{x} : G(\mathbf{x}) = 0 \}$ .

Find: The control history  $\mathbf{u}^*(t)$ ,  $0 \leq t \leq t_f$ , that minimizes the cost functional

$$J(\mathbf{u}) = \Phi[\mathbf{x}(t_f), t_f] + \int_0^{t_f} f_0(\mathbf{x}(t), \mathbf{u}(t)) dt \quad (25)$$

(Note that this statement of the theory uses a Bolza performance index for generality. For the orbital plane change problem,  $f_0$  is zero.)

## B. THE BASIC MAXIMUM PRINCIPLE

The Basic Maximum Principle (BMP) covers the above problem in the absence of the state constraint d). This principle will be stated first and then modified to form the Restricted Maximum Principle (RMP).

Define for  $\lambda \in \mathbb{R}^n$

$$H(\mathbf{x}, \mathbf{u}, \lambda) = -f_0(\mathbf{x}, \mathbf{u}) + \lambda \cdot \mathbf{f}(\mathbf{x}, \mathbf{u}) \quad (26)$$

(H is called the Hamiltonian) and

$$M(\mathbf{x}, \lambda) = \max_{\mathbf{u} \in U} H(\mathbf{x}, \mathbf{u}, \lambda) \quad (27)$$

Then the principle can be stated as: [Ref. Pontryagin see Knowles page 57 [4]]

Suppose  $\mathbf{u}^*$  is an optimal control for the above problem and  $\mathbf{x}^*$  is the corresponding trajectory. Then there exists a non-vanishing function  $\lambda^*(t)$ , hereafter referred to as costates, such that

$$(i) \quad \dot{\mathbf{x}}^* = \mathbf{f}(\mathbf{x}^*, \mathbf{u}^*) \quad (28)$$

$$(ii) \quad \dot{\lambda}^* = -\frac{\partial H}{\partial \mathbf{x}} \quad (29)$$

$$(iii) \quad H(\mathbf{x}^*, \mathbf{u}^*, \lambda^*) = M(\mathbf{x}^*, \lambda^*) = \max_{\mathbf{u} \in U} H(\mathbf{x}^*, \mathbf{u}, \lambda^*) \quad (30)$$

The boundary conditions to be satisfied by the above  $2n$  dimensional system of first order ODE's are given by  $\mathbf{x}_0, \mathbf{F}=\mathbf{0}$ , and the terminal transversality conditions:

$$\lambda(t_f) = - \left( \frac{\partial \Phi}{\partial \mathbf{x}} + \left( \frac{\partial \mathbf{F}}{\partial \mathbf{x}} \right)^T \mathbf{v} \right)_{t=t_f} \quad (31)$$

$$H(t_f) = \left( \frac{\partial \Phi}{\partial t} + \left( \frac{\partial \mathbf{F}}{\partial t} \right)^T \mathbf{v} \right)_{t=t_f} \quad (32)$$

### C. THE RESTRICTED MAXIMUM PRINCIPLE

Now, restrict the control problem further applying d) from above. In particular, suppose the set of admissible controls  $\mathbf{U}$  is the set of all  $\mathbf{u} \in \mathbf{R}^s$  for which:

$$b_1(\mathbf{u}) \leq 0, b_2(\mathbf{u}) \leq 0, \dots, b_k(\mathbf{u}) \leq 0, \quad (33)$$

for given continuously differentiable functions  $b_1, b_2, \dots, b_k$ . in particular  $\mathbf{U}=[-1,1]$  could be written

$$\{u \in \mathbf{R}: u^2 - 1 \leq 0\}, \quad (34)$$

that is

$$b_1(u) = u^2 - 1, \quad u \in \mathbf{R}. \quad (35)$$

If we define

$$p(\mathbf{x}, \mathbf{u}) = \nabla_{\mathbf{x}} G(\mathbf{x}) \cdot \mathbf{f}(\mathbf{x}, \mathbf{u}), \quad (36)$$

then once a trajectory  $\mathbf{x}(t)$  with control  $\mathbf{u}(t)$ , hits the boundary of  $B$ ,  $G(\mathbf{x})=0$ , a necessary and sufficient condition for it to remain there for all later  $t$  is that

$$p(\mathbf{x}(t), \mathbf{u}(t)) = 0. \quad (37)$$

This asserts just that the velocity of a point moving along the trajectory is tangent to the boundary at time  $t$ . Two further assumptions that will be required later are that

$$\nabla_{\mathbf{u}} p(\mathbf{x}, \mathbf{u}) \neq 0, \quad (38)$$

and that

$$\nabla_{\mathbf{u}} p(\mathbf{x}, \mathbf{u}), \nabla_{\mathbf{u}} b_1(\mathbf{u}), \dots, \nabla_{\mathbf{u}} b_k(\mathbf{u}) \quad (39)$$

be linearly independent, on the boundary of  $B$ , along an optimal trajectory  $\mathbf{x}^*(t), \mathbf{u}^*(t)$ .

This ensures that

$$k+1 \leq s \quad (40)$$

The strategy for solving state constrained problems is to break them into two sub-problems. Whenever the optimum trajectory  $\mathbf{x}^*(t)$  lies in the interior of  $B$ ,  $G(\mathbf{x}^*(t)) < 0$ , the state constraints are superfluous (non-binding), and the BMP is applied. However, as soon as  $\mathbf{x}^*(t)$  hits the boundary,  $G(\mathbf{x}^*(t)) = 0$ , the RMP is applied. In this way, as long as  $\mathbf{x}^*$  consists of a finite number of pieces of these two types, there is hope to construct it. The essential point of the RMP is that once the boundary is contacted, the control power must be limited to prevent the optimum trajectory from leaving  $B$ . From the above remarks, this requires that the optimal control  $\mathbf{u}^*(t)$  not only take on values in  $U$ , but also that

$$p(\mathbf{x}^*(t), \mathbf{u}^*(t)) = 0 \quad (41)$$

Define also

$$L = H - \sum \kappa_i b_i - \eta p, \quad (42)$$

( $L$  is called the Lagrangian where  $\eta(t), \kappa_1(t), \dots, \kappa_r(t)$ , are Lagrange multipliers)

The RMP takes into account the added control restraint of Equation (41) and can be stated as:

Let  $\mathbf{x}^*(t)$ ,  $t_0 \leq t \leq t_1$ , be an optimal trajectory with control  $\mathbf{u}^*(t)$ , and suppose that  $\mathbf{x}^*(t)$  lies entirely on the boundary of  $B$ ,  $t_0 \leq t \leq t_1$ , and Equations (38)-(41) are satisfied. Then there exists a continuous vector function  $\lambda(t)$  and a piecewise smooth scalar function  $\eta(t)$ ,  $t_0 \leq t \leq t_1$ , such that

$$(i) \quad \dot{\mathbf{x}}^* = \mathbf{f}(\mathbf{x}^*, \mathbf{u}^*), \quad (43)$$

$$(ii) \quad \dot{\lambda}^* = -\frac{\partial L}{\partial \mathbf{x}} = -\nabla_{\mathbf{x}} H(\mathbf{x}^*, \mathbf{u}^*, \lambda) + \eta(t) \nabla_{\mathbf{x}} p(\mathbf{x}^*, \mathbf{u}^*) \quad (44)$$

$$(iii) H(\mathbf{x}^*, \mathbf{u}^*, \lambda) = M(\mathbf{x}^*, \lambda) = \max_{\mathbf{u} \in U} H(\mathbf{x}^*, \mathbf{u}, \lambda) \quad (45)$$

for  $t_0 \leq t \leq t_1$ , where the maximum is taken subject to  $\mathbf{u} \in U$ , that is, Equations (33) and (37). Since this is really just a constrained maximization, Equation (45) can be alternatively written

$$(iv) \nabla_{\mathbf{u}} L = \mathbf{0} = \nabla_{\mathbf{u}} H(\mathbf{x}^*, \mathbf{u}^*, \lambda^*) - \eta(t) \nabla_{\mathbf{u}} p(\mathbf{x}^*, \mathbf{u}^*) - \sum_{i=1}^k \kappa_i b_i(\mathbf{u}^*) \quad (46)$$

$t_0 \leq t \leq t_1$ , at least at points of differentiability of  $\eta$ .

$$(v) \lambda(t_0) \neq 0 \quad (47)$$

and  $\lambda(t_0)$  is tangent to the boundary of  $B$  at  $\mathbf{x}^*(t)$ .

(vi) Whenever  $\eta$  is differentiable  $\dot{\eta}(t) \nabla g(\mathbf{x}^*(t))$  is directed toward the interior of  $B$  or is zero.

From the assumptions of Equations (38)-(41), (iv) can be discussed in more detail. At any point of continuity of  $\eta$ , for given  $\mathbf{x}^*(t)$ ,  $\mathbf{u}^*(t)$ , and  $\lambda(t)$ , (iv) is a system of  $s$  equations in  $k+1$  unknowns  $\eta(t), \kappa_1(t), \dots, \kappa_k(t)$ . Assumptions (38) and (39) guarantee that the matrix of the system has rank  $k+1$ , and so the unknowns can be solved for; in particular  $\eta$  can be solved for as

$$\eta(t) = \lambda(t) \cdot \mathbf{a}(t), \quad t_0 \leq t \leq t_1, \quad (48)$$

where  $\mathbf{a}$  is a piecewise smooth function. An important point here is that with a state constraint in the problem  $k+1$  must be less than or equal to  $s$  in order to solve the system, limiting the number of control constraint functions allowed.

The boundary conditions for the differential system in the RMP not changed by the state constraint. What is changed here is the dynamics of the system that must meet the boundary conditions.

#### D. JUMP CONDITIONS

As pointed out above, the strategy for constructing the optimal trajectory is to find a finite sequence of alternating subarcs which are either not affected by the state constraint or lie along the boundary of the constraint. This will require the subarcs to be connected. At these connecting points additional conditions are imposed on the optimal trajectory. These additional conditions are called 'jump conditions' because they

potentially force the costates to have a jump discontinuity upon exit from the boundary of B. The costates are assumed to be continuous upon entering the constrained arc and then a modification must be made to the costate values on exiting the constrained arc. If  $t_a$  is the time the constraint is encountered and  $t_b$  is the time that the constrained arc is terminated the jump conditions are as follows:

$$\lambda(t_a - 0) = \lambda(t_a + 0), \quad (49)$$

$$\lambda(t_b + 0) = \lambda(t_b - 0) - \eta(t_b) \nabla_x G(\mathbf{x}(t_b)) \quad (50)$$

## E. THE COMPLETE FORMULATION

In order to generate a complete trajectory from  $t = 0$  to  $t = t_f$ , the equations would be propagated as an unconstrained arc applying the Basic Maximum Principle until the boundary was reached. At that time the equations would be propagated using the RMP and upon leaving the boundary of B the jump conditions would be applied to the costates and the equations would continue applying the basic principle again, etc. By this method a series of alternating arcs is generated which when satisfying all of the boundary conditions produces the optimal trajectory.

A note about the Lagrange multipliers mentioned in the RMP. The Lagrange multipliers have the property that they are zero when the associated constraint is not binding and non-zero when the constraint function is equal to zero. In the case of  $\eta$ ,  $\eta=0$  implies that  $G(\mathbf{x}^*(t)) < 0$  which is when the basic principle is applied and  $\eta$  is non-zero when  $G(\mathbf{x}^*(t)) = 0$  and the RMP is applied. The  $\kappa$ 's have this property relative to their associated  $q$  as well as the restriction that they be positive when their associated  $q=0$ . This can be written as

$$\eta p = 0 \quad (51)$$

$$\kappa_i b_i = 0 \quad (52)$$

$$\kappa_i \geq 0 \quad (53)$$

$$b_i \leq 0 \quad (54)$$

This property is sometimes referred to as complimentary slackness.

So, at this point there is a  $2n$  dimensional system of first order ODE's. The  $2n+1$  boundary conditions are provided by  $n$  initial conditions  $\mathbf{x}_0$ ,  $m$  target conditions from  $\mathbf{F}(\mathbf{x}(t_f), t_f) \in \mathbf{R}^m$ , and the remaining  $n+1-m$  conditions come from the terminal transversality conditions. The costate equations have jump discontinuities as they exit the constrained arcs which are specified by the jump conditions. The difficult task at this point, as is almost always the case when using indirect methods, is solving this two point boundary value problem (TPBVP).

## F. APPLICATION OF THE RESTRICTED MAXIMUM PRINCIPLE

Now the above theory will be applied to the atmospheric pass of the problem at hand. The state vector is modified to

$$\mathbf{x} = [r \quad v \quad \gamma \quad \phi \quad \psi \quad m]^T \quad (55)$$

i.e., the  $\theta$  state is left out. This is because it turns out that the  $\theta$ -costate,  $\lambda_\theta$ , is identically zero for the entire trajectory during both the constrained and unconstrained portions. This comes from the fact that the  $\theta$ -costate derivative is identically zero and the terminal transversality condition gives the  $\theta$ -costate a value of zero at the terminal time making this costate identically zero. Since the  $\theta$ -costate is zero and  $\theta$  does not appear in any other state derivatives, it need not be calculated in determining the optimal control for this problem. It can be computed after the final iteration from the other states if needed to visualize the trajectory. This reduces the problem from 14 equations to 12 and significantly simplifies the remaining costate derivatives. For applying the RMP we have the following:

The cost functional:

$$J = \cos(i(t_f)) = \Phi[\mathbf{x}(t_f), t_f] = \cos(\phi(t_f))\cos(\psi(t_f)) \quad (56)$$

Note that  $f_0 = 0$  in this case.

The costate vector:

$$\lambda = [\lambda_r \quad \lambda_v \quad \lambda_\gamma \quad \lambda_\phi \quad \lambda_\psi \quad \lambda_m]^T \quad (57)$$

The control vector:

$$\mathbf{u} = [T, \alpha, \delta]^T \quad (58)$$

The admissible controls:

$$U = \{ \mathbf{u} : 0 \leq T \leq T_{\max}, 0 \leq \alpha \leq \alpha_{\max} \} \quad (59)$$

The control constraint function:

The constraints on  $T$  and  $\alpha$  could be represented by two functions:

$$b_1 = T^2 - TT_{\max} \quad (60)$$

and

$$b_2 = \alpha^2 - \alpha\alpha_{\max} \quad (61)$$

However, in this case, as will be seen later in Equation (92), the derivative of  $L$  with respect to  $\delta$  does not contain any of the Lagrange multipliers. This effectively reduces the number of equations in the system to be solved to 2. This means that we are only allowed two Lagrange multipliers if the system is to be solved. Thus, we must find one function which encompasses all of the constraints on  $T$  and  $\alpha$ . Suppose we define  $b$  as

$$b = \left( \frac{2T}{T_{\max}} - 1 \right)^z + \left( \frac{2\alpha}{\alpha_{\max}} - 1 \right)^z - 1 \quad (62)$$

where  $z$  is large, positive, and even. This exponent causes the function to take on a value of almost exactly -1 whenever  $0 < T < T_{\max}$  and  $0 < \alpha < \alpha_{\max}$ , and a value of almost exactly 0 when either control is at its boundary with the other in the interior. The value of  $b$  is very large and positive when any control is outside the allowed region. By choosing  $z$  arbitrarily large (e.g.  $z = 200$ ) this function can be made to come arbitrarily close to the corners of the region. The following figures will demonstrate the effect of increasing  $z$ . For each value of  $z$  two plots are shown. The first is a 3-d view of the function shape. The second is a 2-d view for the angle of attack side of the function.



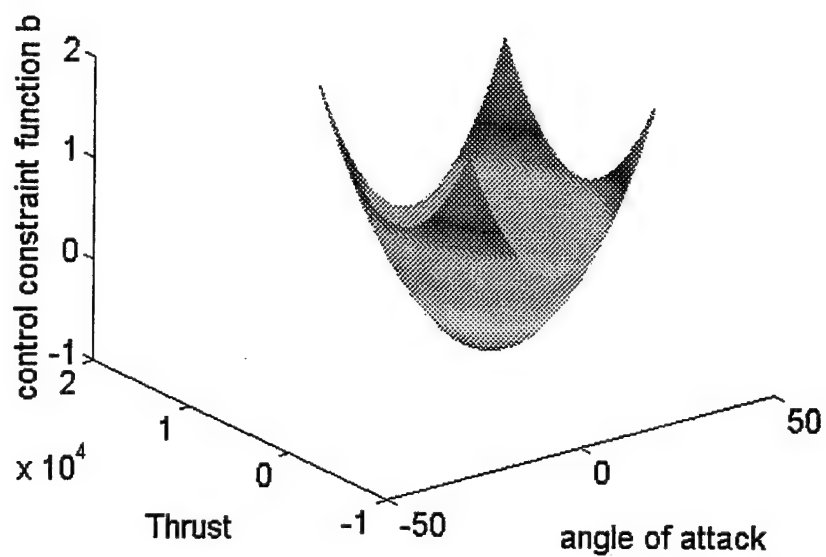


Figure 9: Constraint Function for  $z=2$

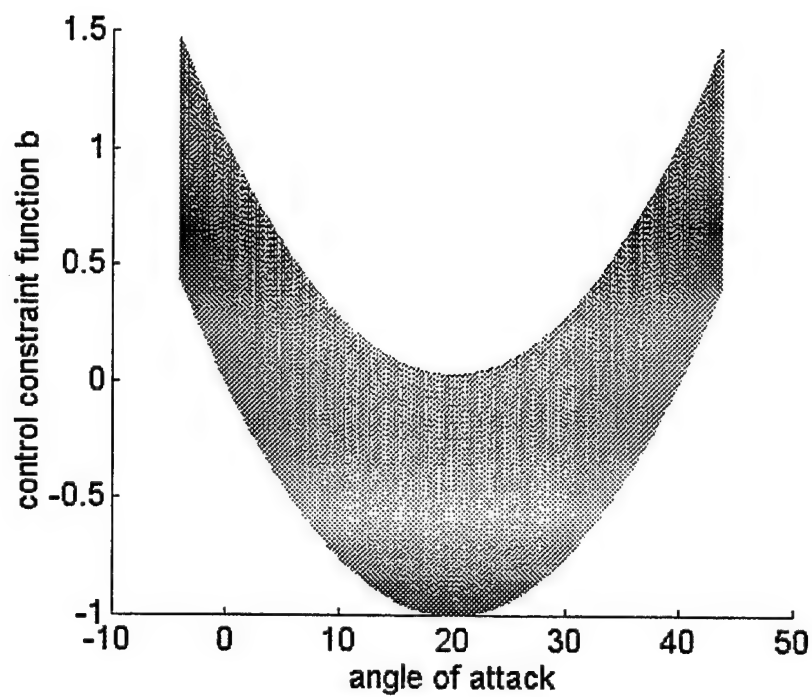


Figure 10: Constraint Function for  $z=2$

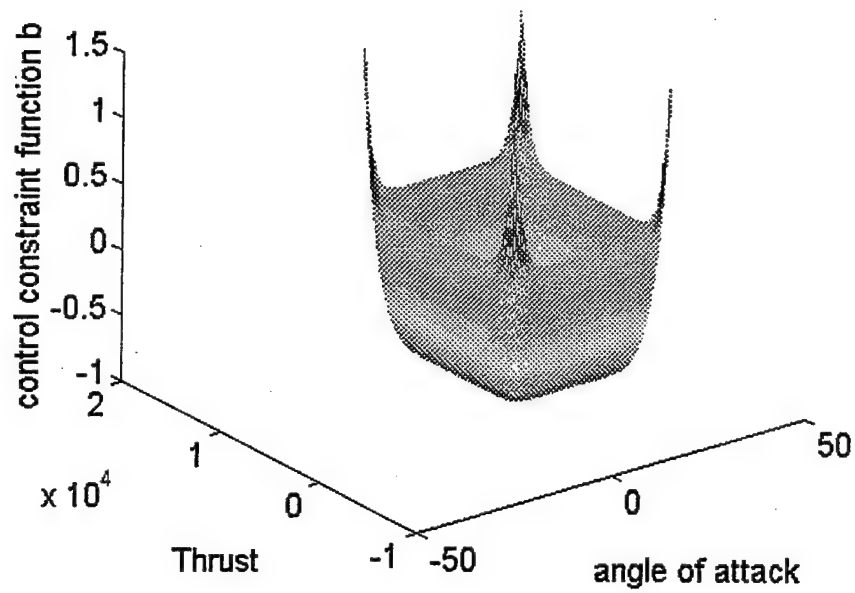


Figure 11: Constraint Function for  $z=10$

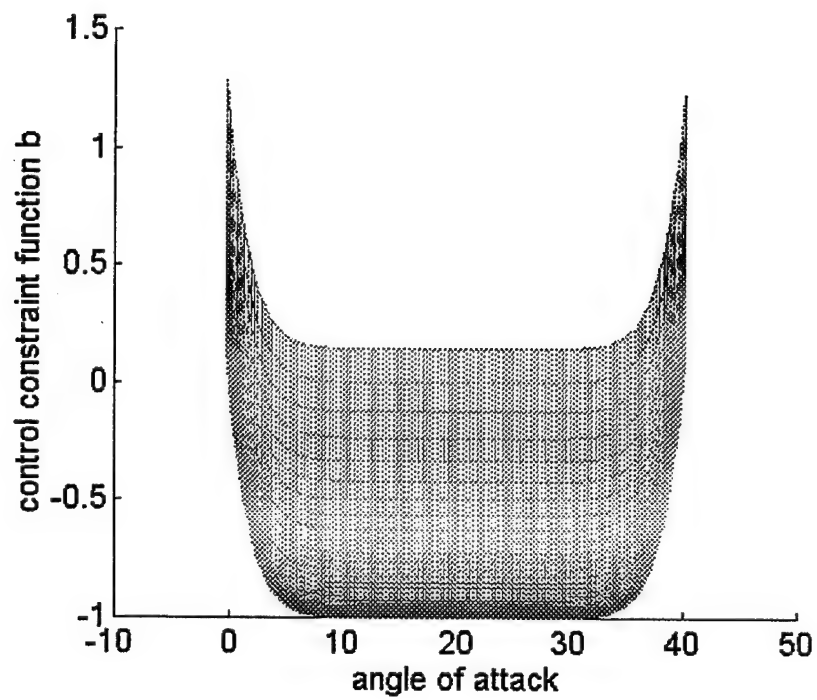


Figure 12: Constraint Function for  $z=10$

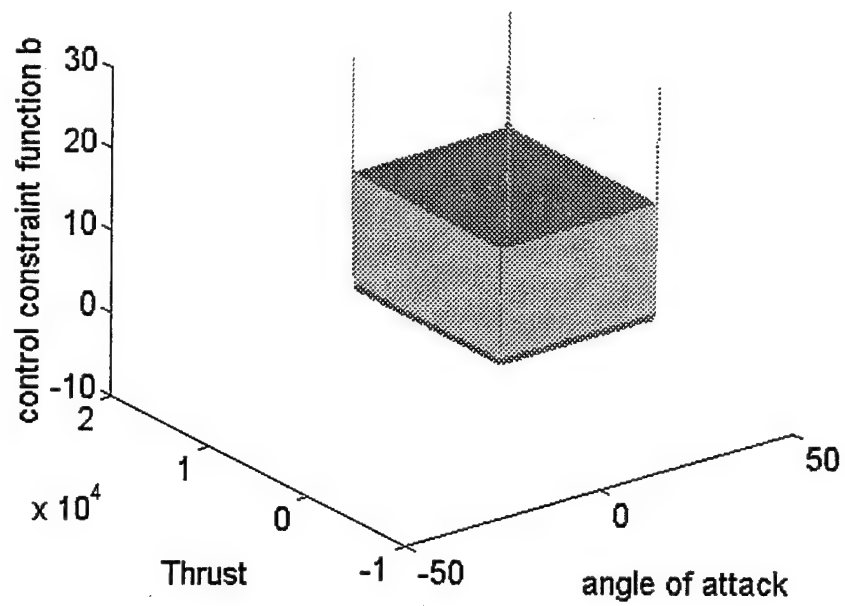


Figure 13: Constraint Function for  $z=200$

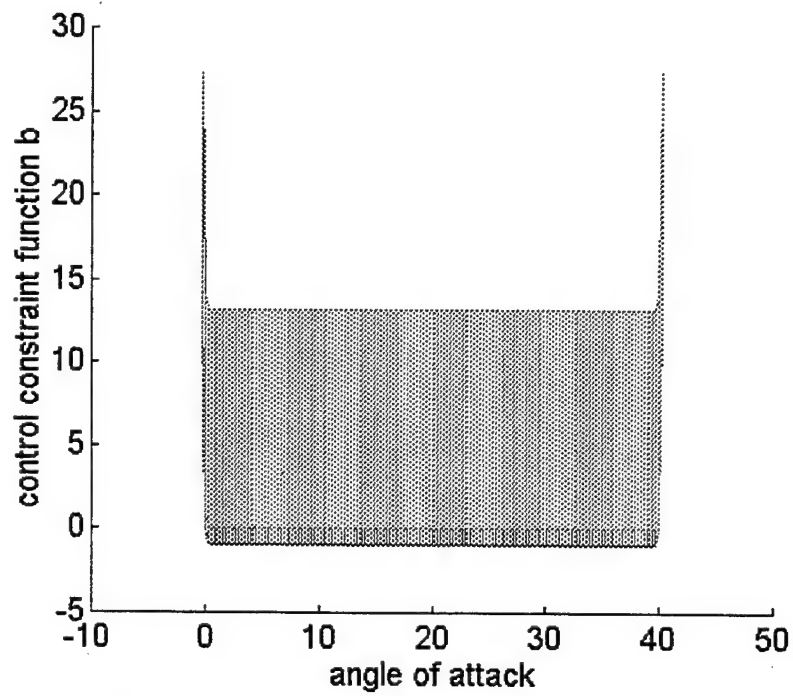


Figure 14: Constraint Function for  $z=200$

The state derivatives:

$$\dot{\mathbf{x}} = \mathbf{f}(\mathbf{x}, \mathbf{u}) \quad (63)$$

As described in the equations of motion in the previous chapter.

The state constraint:

$$\dot{q} = C \rho^{0.5} v^{3.15} \leq \dot{q}_{\max} \quad (64)$$

The state constraint function ( $G \leq 0 \Rightarrow \dot{q} \leq \dot{q}_{\max}$ ):

$$G = C \rho_0 e^{(-\beta N(r-r_0))} v^M - \dot{q}_{\max} \quad (65)$$

where  $N=5$ ,  $M=3.15$  and  $\dot{q}_{\max}$  is a positive constant.

The boundary function ( $p = 0 \Rightarrow \dot{q} = \text{const}$ ):

$$p = \nabla_x G \cdot \mathbf{f}(\mathbf{x}, \mathbf{u}) \quad (66)$$

$$p = T \cos(\alpha) - D(\alpha) - m \sin(\gamma) \left( \frac{\mu}{r^2} + \xi v^2 \right) \quad (67)$$

where

$$\xi = \frac{5\beta}{3.15} \quad (68)$$

The Lagrangian: ( $L = \lambda \cdot \mathbf{f}(\mathbf{x}, \mathbf{u}) - \kappa b - \eta p$ ):

$$\begin{aligned} L = & \lambda_r v \sin(\gamma) + \lambda_v \left( \frac{T \cos(\alpha) - D(\alpha)}{m} - \frac{\mu \sin(\gamma)}{r^2} \right) \\ & + \frac{\lambda_\gamma \left( \frac{(L(\alpha) + T \sin(\alpha)) \cos(\delta)}{m} - \frac{\mu \cos(\gamma)}{r^2} + \frac{v^2 \cos(\gamma)}{r} \right)}{v} + \frac{\lambda_\phi v \cos(\gamma) \sin(\psi)}{r} \\ & + \frac{\lambda_\psi \left( \frac{(L(\alpha) + T \sin(\alpha)) \sin(\delta)}{m \cos(\gamma)} - \frac{v^2 \cos(\gamma) \cos(\psi) \tan(\phi)}{r} \right)}{v} - \frac{\lambda_m T}{Isp g_0} \\ & - \kappa \left( \left( 2 \frac{T}{T_{\max}} - 1 \right)^2 + \left( 2 \frac{\alpha}{\alpha_{\max}} - 1 \right)^2 - 1 \right) - \eta \left( T \cos(\alpha) - D(\alpha) - m \sin(\gamma) \left( \frac{\mu}{r^2} + \xi v^2 \right) \right) \end{aligned} \quad (69)$$

The costate derivatives :  $(\dot{\lambda} = -\frac{\partial L}{\partial x})$

$$\begin{aligned} \frac{d\lambda_r}{dt} = & -2 \frac{\lambda_v \mu \sin(\gamma)}{r^3} - \frac{\lambda_\gamma \left( 2 \frac{\mu \cos(\gamma)}{r^3} - \frac{v^2 \cos(\gamma)}{r^2} \right)}{v} + \frac{\lambda_\phi v \cos(\gamma) \sin(\psi)}{r^2} \\ & - \frac{\lambda_\psi v \cos(\gamma) \cos(\psi) \tan(\phi)}{r^2} + 2 \frac{\eta m \sin(\gamma) \mu}{r^3} \end{aligned} \quad (70)$$

$$\begin{aligned} \frac{d\lambda_v}{dt} = & -\lambda_r \sin(\gamma) - 2 \frac{\lambda_\gamma \cos(\gamma)}{r} + \frac{\lambda_\gamma \left( \frac{(L(\alpha) + T \sin(\alpha)) \cos(\delta)}{m} - \frac{\mu \cos(\gamma)}{r^2} + \frac{v^2 \cos(\gamma)}{r} \right)}{v^2} \\ & - \frac{\lambda_\phi \cos(\gamma) \sin(\psi)}{r} + 2 \frac{\lambda_\psi \cos(\gamma) \cos(\psi) \tan(\phi)}{r} \\ & + \frac{\lambda_\psi \left( \frac{(L(\alpha) + T \sin(\alpha)) \sin(\delta)}{m \cos(\gamma)} - \frac{v^2 \cos(\gamma) \cos(\psi) \tan(\phi)}{r} \right)}{v^2} - 2 \eta m \sin(\gamma) \xi v \end{aligned} \quad (71)$$

$$\begin{aligned} \frac{d\lambda_\gamma}{dt} = & -\lambda_r v \cos(\gamma) + \frac{\lambda_v \mu \cos(\gamma)}{r^2} - \frac{\lambda_\gamma \left( \frac{\mu \sin(\gamma)}{r^2} - \frac{v^2 \sin(\gamma)}{r} \right)}{v} + \frac{\lambda_\phi v \sin(\gamma) \sin(\psi)}{r} \\ & - \frac{\lambda_\psi \left( \frac{(L(\alpha) + T \sin(\alpha)) \sin(\delta) \sin(\gamma)}{m \cos(\gamma)^2} + \frac{v^2 \sin(\gamma) \cos(\psi) \tan(\phi)}{r} \right)}{v} \\ & - \eta m \cos(\gamma) \left( \frac{\mu}{r^2} + \xi v^2 \right) \end{aligned} \quad (72)$$

$$\frac{d\lambda_\phi}{dt} = \frac{\lambda_\psi v \cos(\gamma) \cos(\psi) (1 + \tan(\phi)^2)}{r} \quad (73)$$

$$\frac{d\lambda_\psi}{dt} = -\frac{\lambda_\phi v \cos(\gamma) \cos(\psi)}{r} - \frac{\lambda_\psi v \cos(\gamma) \sin(\psi) \tan(\phi)}{r} \quad (74)$$

$$\begin{aligned} \frac{d\lambda_m}{dt} = & \frac{\lambda_v (T \cos(\alpha) - D(\alpha))}{m^2} + \frac{\lambda_\gamma (L(\alpha) + T \sin(\alpha)) \cos(\delta)}{m^2 v} + \frac{\lambda_\psi (L(\alpha) + T \sin(\alpha)) \sin(\delta)}{m^2 \cos(\gamma) v} \\ & - \eta \sin(\gamma) \left( \frac{\mu}{r^2} + \xi v^2 \right) \end{aligned} \quad (75)$$

The initial state vector  $\mathbf{x}_0$  is completely specified as discussed in the overall problem statement. The initial states are all determined by the exoatmospheric portion of the descent. The choice of  $\sigma_{deorbit}$  and  $\Delta V_{deorbit}$  will specify the atmospheric entry states.

The target function:

$$\mathbf{F}(\mathbf{x}(t_f), t_f) = \begin{bmatrix} \gamma_{exit} - \gamma(t_f) \\ R_{atm} - r(t_f) \\ V_{exit} - v(t_f) \\ m_{exit} - m(t_f) \end{bmatrix} \quad (76)$$

These conditions are specified by the reorbit and circularization impulses and bank angles chosen.

The terminal transversality conditions:  $(\lambda(t_f) = -\left( \frac{\partial \Phi}{\partial \mathbf{x}} + \left( \frac{\partial \mathbf{F}}{\partial \mathbf{x}} \right)^T \mathbf{v} \right)_{t=t_f})$

$$\lambda_r(t_f) = v_1 \quad (77)$$

$$\lambda_v(t_f) = v_2 \quad (78)$$

$$\lambda_\gamma(t_f) = v_3 \quad (79)$$

$$\lambda_\phi(t_f) = \sin(\phi(t_f)) \cos(\psi(t_f)) \quad (80)$$

$$\lambda_\psi(t_f) = \cos(\phi(t_f)) \sin(\psi(t_f)) \quad (81)$$

$$\lambda_m(t_f) = v_4 \quad (82)$$

The above equations yield two non-linear boundary conditions in (80) and (81)

$$\text{The terminal Hamiltonian value: } (H(t_f) = \left( \frac{\partial \Phi}{\partial t} + \left( \frac{\partial \mathbf{F}}{\partial t} \right)^T \mathbf{v} \right)_{t=t_f})$$

$$H(t_f) = 0 \quad (83)$$

It should be noted here that in value the Hamiltonian and the Lagrangian are equal. So, this is equivalent to making the Lagrangian zero at  $t_f$ .

Thus there are 13 boundary conditions for the 12 equations which are necessary to be satisfied by the optimal solution. The 13<sup>th</sup> is necessary because the terminal time is unknown. It is possible with a change of dependent variable and the addition of an additional parameter, namely the terminal time, to cause the system to always be integrated between 0 and 1. This is done by letting  $\tau = t/t_f$ , the new dependent time variable  $\tau$ , is then the variable of integration and all 12 of the differential equations have their right hand sides multiplied by  $t_f$ . This in essence scales all the equations into the 0 to 1 time frame. This is a good idea here since it simplifies the boundary value problem by fixing the terminal time at 1 at the cost of only one additional parameter in the parameter optimization process going on external to the boundary value solver.

The jump conditions show how the costate variables must jump when exiting the boundary region during the integration.

The jump conditions:  $(\lambda(t_b + 0) = \lambda(t_b - 0) - \eta(t_b) \nabla_x G(\mathbf{x}(t_b)))$

$$\lambda_r(t_b + 0) = \lambda_r(t_b - 0) + \eta C \rho_0 \beta N e^{(-\beta N(r - r_0))} v^M \quad (84)$$

$$\lambda_v(t_b + 0) = \lambda_v(t_b - 0) - \frac{\eta C \rho_0 e^{(-\beta N(r - r_0))} v^M M}{v} \quad (85)$$

$$\lambda_\gamma(t_b + 0) = \lambda_\gamma(t_b - 0) \quad (86)$$

$$\lambda_\phi(t_b + 0) = \lambda_\phi(t_b - 0) \quad (87)$$

$$\lambda_{\psi}(t_b + 0) = \lambda_{\psi}(t_b - 0) \quad (88)$$

$$\lambda_m(t_b + 0) = \lambda_m(t_b - 0) \quad (89)$$

Here again it can be seen that the value of  $\eta$  is needed to perform the integration. Also note that the only costates affected are those whose respective states appear in  $G$ . The remaining costates are continuous at both entry to and exit from a constrained arc.

The determination of the value of  $\eta$  and of the optimal controls go hand in hand. The necessary conditions on the controls are:

$$\frac{\partial L}{\partial u} = 0 \quad (90)$$

$$\frac{\partial}{\partial T} L =$$

$$\frac{\lambda_v \cos(\alpha)}{m} + \frac{\lambda_{\gamma} \sin(\alpha) \cos(\delta)}{m v} + \frac{\lambda_{\psi} \sin(\alpha) \sin(\delta)}{m \cos(\gamma) v} - \frac{\lambda_m}{Isp g_0} - 2 \frac{\kappa \left( 2 \frac{T}{T_{max}} - 1 \right)^z}{T_{max} \left( 2 \frac{T}{T_{max}} - 1 \right)} - \eta \cos(\alpha) \quad (91)$$

$$\frac{\partial}{\partial \delta} L = - \frac{\lambda_{\gamma} (L(\alpha) + T \sin(\alpha)) \sin(\delta)}{m v} + \frac{\lambda_{\psi} (L(\alpha) + T \sin(\alpha)) \cos(\delta)}{m \cos(\gamma) v} \quad (92)$$

$$\begin{aligned} \frac{\partial}{\partial \alpha} L = & \frac{\lambda_v \left( -T \sin(\alpha) - \left( \frac{\partial}{\partial \alpha} D(\alpha) \right) \right)}{m} + \frac{\lambda_{\gamma} \left( \left( \frac{\partial}{\partial \alpha} L(\alpha) \right) + T \cos(\alpha) \right) \cos(\delta)}{m v} \\ & + \frac{\lambda_{\psi} \left( \left( \frac{\partial}{\partial \alpha} L(\alpha) \right) + T \cos(\alpha) \right) \sin(\delta)}{m \cos(\gamma) v} - 2 \frac{\kappa \left( 2 \frac{\alpha}{\alpha_{max}} - 1 \right)^z}{\alpha_{max} \left( 2 \frac{\alpha}{\alpha_{max}} - 1 \right)} - \eta \left( -T \sin(\alpha) - \left( \frac{\partial}{\partial \alpha} D(\alpha) \right) \right) \end{aligned} \quad (93)$$



From Equation (92) a relationship for the optimal bank angle can be derived:

$$\delta = \arctan \left( \frac{\lambda_{\psi}}{\lambda_{\gamma} \cos(\gamma)} \right) \quad (94)$$

This relationship holds for the entire trajectory, both on constrained and unconstrained arcs.

Equations (91), (93), (37) and the complementary slackness property given in Equations (51) through (54) will then form a system of equations in the unknowns needed to determine the optimal values of  $T$ ,  $\alpha$ ,  $\kappa$ , and  $\eta$ . A difficulty could arise if  $\kappa$  were allowed to be zero for any finite time. The difficulty is that any value of  $T$  would satisfy these conditions. It can be observed that, in Equation (91),  $T$  cannot be evaluated if  $\kappa=0$ . When the second derivative of  $L$  with respect to  $T$  is considered, it can be seen that the second order condition for maximizing  $L$  with respect to  $T$  can only be satisfied when  $\kappa>0$ . This is the case when  $b=0$ .

$$\frac{\partial^2 L}{\partial T^2} = \frac{-4\kappa \left( \frac{2T}{T_{\max}} - 1 \right)^{z-2} z(z-1)}{T_{\max}^2} \quad (95)$$

Barring the possibility of  $\kappa=0$ , which would allow any value of  $T$  to be optimal and lead to a so-called singular arc, the constrained arcs which meet these conditions (i.e.,  $b=0$  and  $p=0$ ) are as follows:

- (1)  $T=0$  with  $\alpha$  satisfying Equation (67) with  $0 \leq \alpha \leq \alpha_{\max}$ .
- (2)  $T=T_{\max}$  with  $\alpha$  satisfying Equation (67) with  $0 \leq \alpha \leq \alpha_{\max}$ .
- (3)  $\alpha=0$  with  $T$  satisfying Equation (67) with  $0 \leq T \leq T_{\max}$ .
- (4)  $\alpha=\alpha_{\max}$  with  $T$  satisfying Equation (67) with  $0 \leq T \leq T_{\max}$ .

In the next chapter a numerical analysis will be performed to show how this information should be incorporated into direct method analysis of this problem.



## IV. NUMERICAL ANALYSIS (DIRECT METHOD)

The previous chapters have given some idea of what can be learned by considering the indirect methods of analysis for this problem. This chapter will discuss a direct method of analysis which takes into account the conditions which must be satisfied by the optimal trajectory. This narrows the possibilities for the direct method search. Only those arcs which are allowed in the indirect method will be considered here in the Aerobang trajectory. The Aerocruise analysis is done for comparison to results obtained in [Ref. 3] which did not take into account the existence of some of the previously mentioned arcs. Many of the parameters of the problem are chosen to allow this comparison. This chapter will also discuss how this direct method of analysis can aid in the solution of the indirect problem. Solving the indirect problem is the only way to actually claim optimality. The drawback to the direct analysis is that no matter how good the trajectory is, there is no way to claim optimality unless that trajectory can be shown to solve the necessary conditions discussed previously.

### A. POST

The program which was used for the direct analysis is the Program to Optimize Simulated Trajectories (POST). POST is a general purpose FORTRAN program for simulating and improving point mass trajectories of aerospace vehicles. The program can be used to examine a wide variety of performance and mission analysis problems for atmospheric and orbital vehicles.

The basic simulation flexibility is achieved by decomposing the trajectory into a logical sequence of simulation segments. These trajectory segments, referred to as phases, enable the trajectory analyst to model both the physical and non-physical aspects of the simulation accurately and efficiently. By segmenting the mission into phases, each phase can be modeled and simulated in a manner most appropriate to that particular flight regime. For example, the planet model, the vehicle model, and simulation options can be changed in any phase to be compatible with the level of detail required in that phase. [Ref. 12]

## B. TRAJECTORY CHARACTERIZATION

The POST program takes a single formatted input file. The specifics of the formatting requirements are discussed in [Ref. 13]. It is sufficient here to say that, as stated above, for POST to perform its optimization, the desired trajectory must be broken down into phases which must occur in order and as such constitute an a priori knowledge of the type of trajectory POST will attempt to optimize. Also included in the POST input file are, the control parameters, any constraints which must be met for any feasible trajectory, and the values of the control parameters to be used as the initial iterate. The term control parameter in this context is used to refer to those parameters which POST is allowed to perturb in its search. Two different models were examined in this thesis for the characterization of the orbital plane change maneuver, one for the Aerobang maneuver and the other for an Aerocruise maneuver. The phase structure will be discussed below for each model with the phases listed in sequential order. The discussion will include the control parameters used in each phase. In both cases, the target was to have zero propellant remaining upon trajectory termination. These models represent the final product and, as will be discussed later, require large amounts of user interface to achieve. Figure 15 shows graphically what is required for the trajectory breakdown with the numbers representing phases of the trajectory.

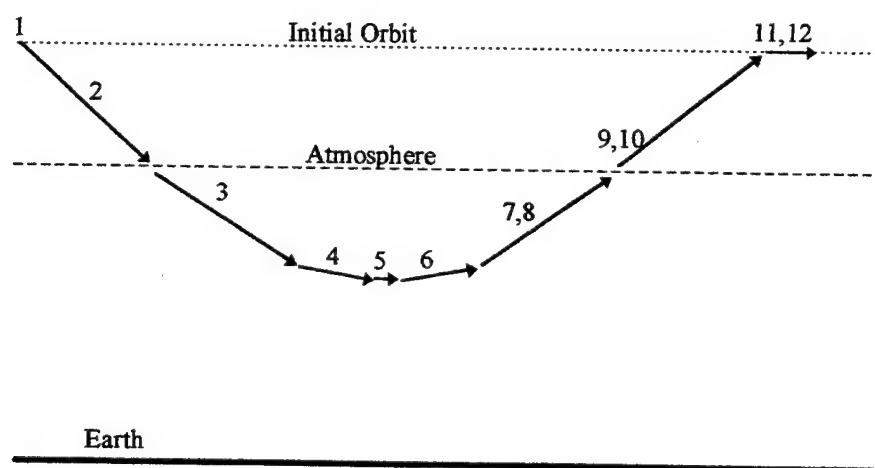


Figure 15: Example Trajectory Characterization (Aerobang)

## **(1) Aerobang phases**

### *Phase 1 Initial Orbit*

The initial orbit for both models is a circular equatorial orbit at 185 km. This initial altitude was chosen for comparison to [Ref. 3]. In this phase the vehicle parameters are also input.

### *Phase 2 Deorbit Impulse*

This phase begins 5 seconds after the orbit is initialized. An impulse in the direction of the negative velocity vector is applied which causes the orbit to become elliptical with apogee at 185 km and perigee less than 111 km, the altitude at which the atmosphere will be 'turned on'. Again, these altitudes were chosen for comparison to [Ref. 3]. The motion is determined with no atmosphere during this phase. The magnitude of the deorbit impulse is a control parameter which POST has at its disposal for its optimization.

### *Phase 3 Atmospheric Entry and Glide to Heating Rate Boundary*

This phase begins when the altitude of the vehicle reaches 111 km. At this point the equations of motion begin to take into account atmospheric forces. The 1962 U.S. standard atmosphere is applied. This atmospheric model was chosen for consistency with [Ref. 3]. Thrust is zero in this phase. The bank angle and angle of attack are used as control parameters by POST. These two controls are represented by a linear polynomial in this phase. POST implements this by using the constant term and the linear term of these two polynomials as control parameters.

### *Phase 4 Zero Thrust Constant Heating Rate Arc*

This phase begins when the heating rate reaches a value equal to the maximum allowed heating rate. During this phase, the thrust is still zero, the angle of attack is modulated according to Equation (37) to keep the heating rate constant. Note that this arc can only be accomplished during a time while the flight path angle is negative which is why this phase is assumed to be the beginning of the heat rate control arc. The angle of bank is a linear polynomial as above with the constant and linear terms used as control parameters. In order for POST to correctly

simulate the constant heating rate arc it was necessary to allow POST to use angles of attack greater than 40 degrees during the iterative process as long as angle of attack was less than 40 degrees for the entire final trajectory. An additional parameter used in the phase is the duration of the arc itself. Thus, POST is allowed to vary the length of this phase.

#### *Phase 5 Max Angle of Attack Transition at Constant Heating Rate*

This phase was included as a result of the transition between the zero thrust and maximum thrust arcs. The thrust is throttled during this phase. As discussed in the theoretical treatment of the problem, this arc must have  $\alpha=0$  or 40 degrees. Since  $\alpha$  is less than 90 degrees, Equation (37) has a jump discontinuity in  $\alpha$  if there is a jump in  $T$ . This is the case in the transition from zero to maximum thrust. It was discovered that this was causing  $\alpha$  to exceed 40 degrees at this transition in the final trajectory. This phase was chosen since it is allowed by the indirect analysis discussed previously and it allows the vehicle to throttle the thrust and build up gradually to maximum thrust while not exceeding the maximum angle of attack. The duration of this phase is very short and its addition resulted in very little change in performance. The angle of attack is 40 degrees and constant during this phase. Bank angle, as a linear polynomial, is used for two control parameters during this phase. Thrust is modulated to maintain the heating rate constant until maximum thrust is reached.

#### *Phase 6 Max Thrust Constant Heating Rate Arc*

This phase begins when the thrust increases to maximum during the transition in phase 5. Thrust is maintained at maximum and  $\alpha$  is modulated to maintain heating rate constant. Bank angle, as a linear polynomial, is used for two control parameters during this phase. The phase duration is also a control parameter in this phase.

#### *Phase 7 Glide to Atmosphere Exit*

This phase begins when the phase duration of phase 6 is reached. The goal of this phase is to reach the top of the atmosphere at 111 km. Thrust is zero unless it becomes apparent that the trajectory will not make it to the top of the atmosphere.

The criteria used to determine this is the flight path angle equal to zero. The phase always begins with a positive flight path angle and if it reaches zero the optional phase 8 is begun. Angle of attack and bank angle, as linear polynomials, are used for four control parameters during this phase.

#### *Phase 8 (Optional) Max Thrust Boost*

This phase begins if the flight path angle reaches zero during phase 7 and takes place concurrently with phase 7. The rocket engine is turned on and the osculating apogee is raised to 185 km. Angle of attack and bank angle are continued as controlled in phase 7. In POST, this event is a sub-event to phase 7 and no direct control is introduced here. POST continues to use the controls it has in phase 7. This phase terminates when the apogee altitude reaches 185 km. And phase 7 continues to the top of the atmosphere.

#### *Phase 9 Atmospheric Exit*

This phase takes place when vehicle altitude reaches 111 km. The atmosphere is turned off and the trajectory continues until altitude reaches 185 km. No control parameters are used during this phase.

#### *Phase 10 Reorbit Impulse*

This phase begins when the flight path angle reaches zero during phase 9 and takes place concurrently with phase 9. The rocket engine is turned on and the osculating apogee is raised to 185 km. This is necessary because the drag from the atmosphere causes the apogee altitude to drop even after the boost maneuver in phase 8. The angle of attack and bank angle are zeroed and the impulse is applied. Since POST cannot apply an impulse whose magnitude depends on the current orbital parameters, it was necessary to approximate an impulse. This is done by using a propulsive rocket firing of 1000 times the magnitude of the normal thrust. This allows the fuel expended during this impulse to be taken into account and the firing to be terminated when the desired orbital parameters are met. This firing takes a very short time, on the order of .1 seconds and closely models a pure impulse. In any case this firing has more losses than an impulse

and is conservative in terms of fuel consumption. No control parameters are associated with this phase.

*Phase 11 Circularization Impulse*

This phase begins when altitude reaches 185 km. A impulsive thrust is applied to circularize the orbit at 185 km. No control parameters are associated with this phase.

*Phase 12 Trajectory Termination*

The trajectory is terminated as soon as the orbit is circularized. POST requires a phase to exist to tell it that the trajectory is ended.

**(2) Aerocruise phases** ( Phases 1-3 are identical for both maneuvers. Aerocruise phases 6-11 are identical to Aerobang phases 7-12.)

*Phase 1 Initial Orbit*

See Aerobang.

*Phase 2 Deorbit Impulse*

See Aerobang.

*Phase 3 Atmospheric Entry and Glide to Flight Leveling Maneuver*

See Aerobang.

*Phase 4 Flight Leveling Maneuver*

This phase begins when a chosen heating rate is achieved. This is one of the parameters that needed to be adjusted manually to target the heating rate desired for the cruise arc. Angle of attack is made maximum and the linear term of the bank angle (bank rate) is used as a control parameter to reduce the bank angle and cause the flight path angle to level to zero for a steady state cruise.

*Phase 5 Steady State Cruise at Constant Heating Rate*

This phase begins when the prescribed flight path angle is reached. Steady cruise requires flight path angle to be identically zero for the entire arc. This is achieved by initiating the arc at zero flight path angle, modulating thrust to drag, and modulating bank angle to maintain  $\dot{\gamma}$  equal to zero. Since POST uses input as look-up tables in which it uses linear interpolation it is not possible to numerically maintain  $\dot{\gamma}$  equal to zero. This results in small changes in flight path



angle and thus altitude and density in the simulated runs. A slightly positive flight path angle was used to initiate this phase in order to spread the numerical error over the entire arc. The variation in heating rate is small, about 1.5 %, and average heating rate on this arc was looked at which is conservative in terms of trajectory performance. Angle of attack is assumed constant for steady state cruise and only this constant term and the phase duration are used as control parameters in this phase.

*Phase 6 Glide to Atmosphere Exit*

See Aerobang.

*Phase 7 Max Thrust Boost*

See Aerobang.

*Phase 8 Atmospheric Exit*

See Aerobang.

*Phase 9 Reorbit Impulse*

See Aerobang.

*Phase 10 Circularization Impulse*

See Aerobang.

*Phase 11 Trajectory Termination*

See Aerobang.

### **C. THE MAN IN THE LOOP**

As alluded to above, working with POST is not a hands-off experience. The user must have a thorough knowledge of the problem being investigated in order to interpret the results. The following is a small list of some examples of the type of intervention required by the user.

- (1) As discussed above, the problem must be set up in phases. This can be done in multiple ways. In [Ref. 1], Nicholson's characterization of the two maneuvers is quite different from what was done here. Many changes were made to 'clean up' the final trajectory produced. The deorbit and circularization impulses were modeled in [Ref. 1] as propulsive retro firings at 180 degrees angle of attack. These were changed to pure impulses. For the

Aerobang problem, the angle of attack required to maintain the heating rate constant is not always less than maximum angle of attack. This can be dealt with in multiple ways. [Ref. 1] began the heat rate control at a time in the trajectory determined by previous runs and limited the angle of attack to maximum. This resulted in not exactly hitting the heating rate and limited the possible trajectories tested for the optimization. This was changed to initiating the heat control phase at the max heating rate and allowing the use of higher values of  $\alpha$  than 40 degrees. An inequality constraint was then placed on the maximum value of  $\alpha$ . This allowed a larger space of potential trajectories. [Ref. 1] did not include the zero thrust heat rate control arc. This was added to again increase the space of trajectories available for the optimization. It was assumed in [Ref. 1] that the atmospheric  $\beta$  was a constant, which is not the case, resulting in non-constant heating rate arcs. This was changed to use the data from the 1962 atmosphere to produce a table for  $\beta$ . There is not necessarily a "right way" or a "wrong way" to set up the trajectory but the results can easily be limited by the users characterization.

- (2) The results of POST's optimization is heavily dependent on the initial trajectory as well as the overall characterization. For instance, if the angle of attack is initially decreasing during the initial glide in the atmosphere, POST searches decreasing angle of attack trajectories, while the opposite is true if the angle of attack is initially chosen to be increasing. This is because POST performs a local maximization of the optimization variable. As a result, POST's final answer may very well be a local extrema and the POST output may indicate that the problem is solved, but the answer may clearly not be the best. For this reason, it was necessary to try various starting point in terms of initial guesses to allow more possibilities to be searched. Another aspect of the initial guess is that sometimes POST's search may lead it to a region were it cannot target the problem. Slight modifications in the initial guess can sometime remedy this situation.

- (3) POST's input can include as many as 25 control variables for a given problem and for this analysis there could be up to 15. However, POST's algorithm becomes even more sensitive to the initial guess the more control parameters it is given to optimize. It was observed that the algorithm became even more local as the number of control parameters was increased. For this reason, it was necessary to perform the optimization in steps. This was done by optimizing the first few phases while fixing the others then fixing the initial phases to those results and moving on to the next few phases. When the entire trajectory had been through this process a few times the changes in the overall trajectory became small. This procedure, although necessary for POST to be more global, does make the problem more user intensive.
- (4) Another area of user intervention is in characterizing the constraints. For instance, the heating rate can be limited as an inequality constraint while only allowable angles of attack are used or the heating rate can be maintained constant using higher than allowable angles of attack with an inequality constraint on  $\alpha$ .

These are only some of the ways a user can have a great affect on the outcome of a direct method optimization, and even after all of this effort, the solution is not optimal unless it can be shown to satisfy those conditions of the RMP. Thus, an in depth knowledge of those conditions can save a user a great deal of work by narrowing the user's effort. An example will be shown later of an instance where the user's characterization of the problem led to not obtaining the best possible solution to the problem.

#### **D. TRAJECTORY RESULTS**

The results obtained in the investigation of the two trajectory characterizations above are shown below. These plots represent the final product of over 100 runs of the POST program. As previously noted the Aerocruise heating rate profile is not exactly constant on the heat rate control arc. The use of a simulation/optimization code which allowed the controls to be input by equations vice look up tables would remedy this problem.

(1) Aerobang plots

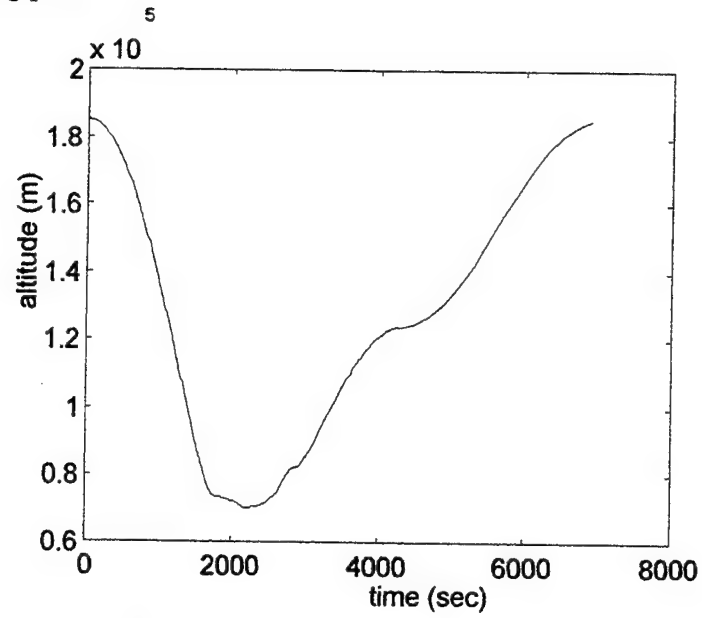


Figure 16: Altitude vs. Time

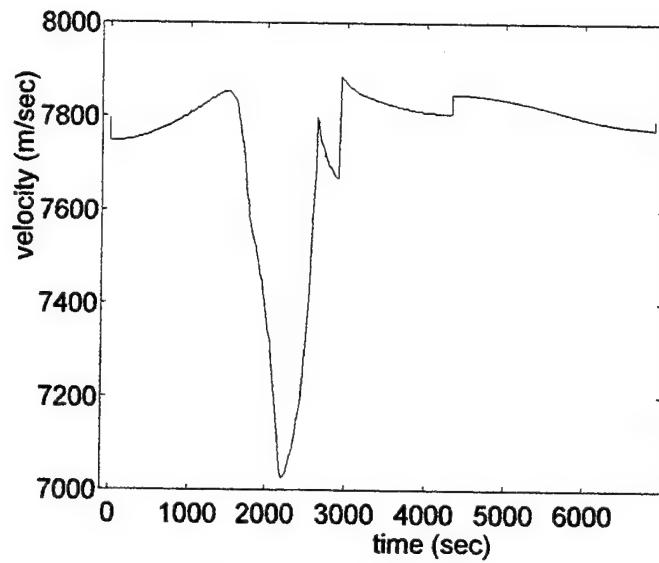


Figure 17: Velocity vs. Time

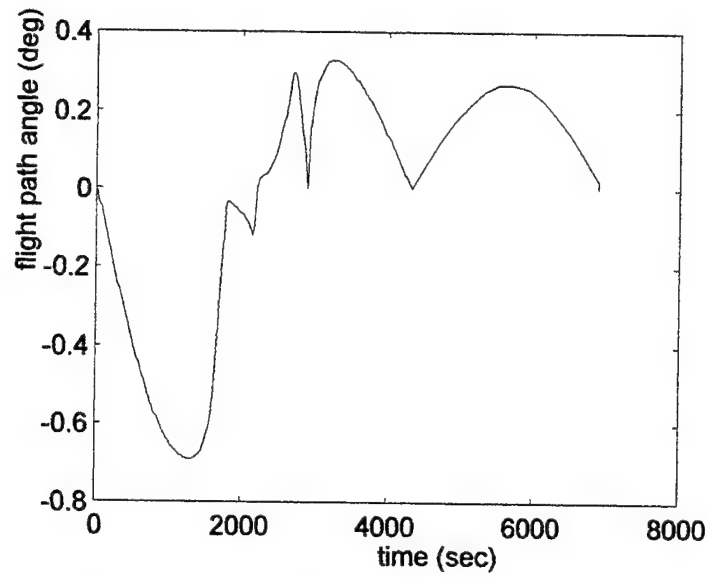


Figure 18: Flight Path Angle vs. Time

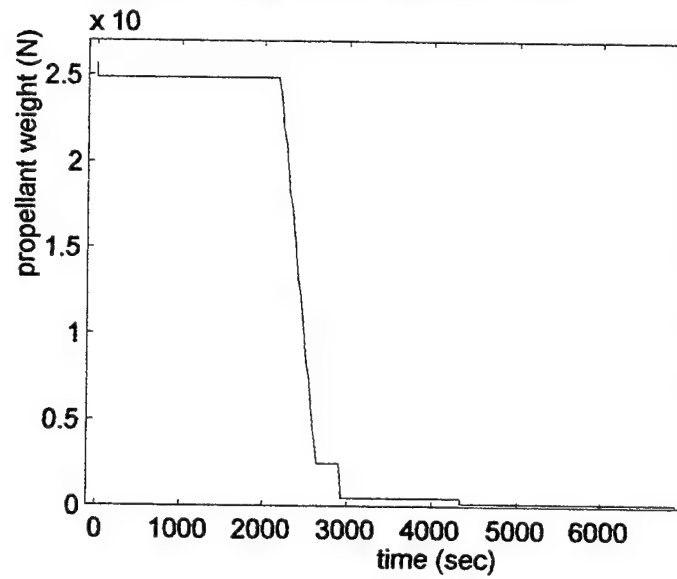


Figure 19: Propellant Weight vs. Time

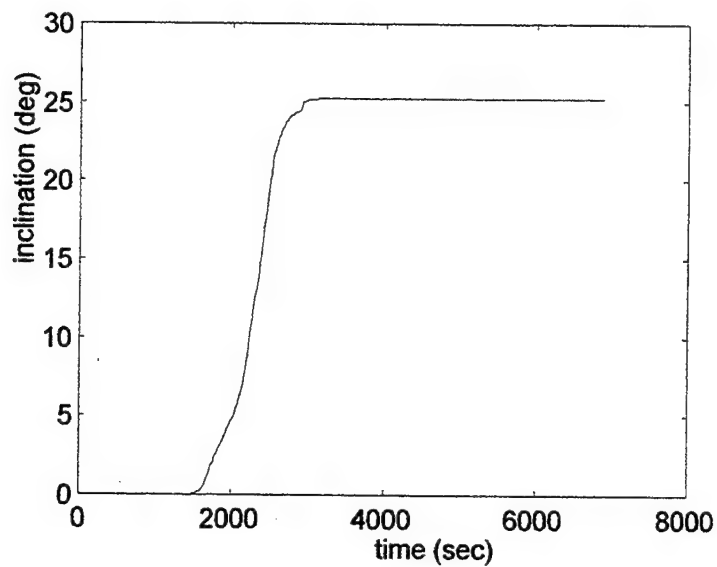


Figure 20: Inclination vs. Time

The above plots show the entire trajectory. The atmosphere is only active below 111 km which corresponds to 1271 to 3641 sec. The remaining plots will show this atmospheric pass only.

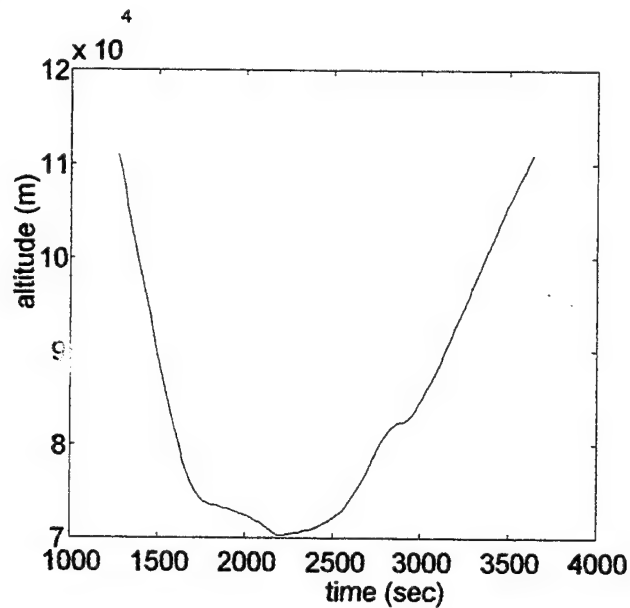


Figure 21: Altitude vs. Time

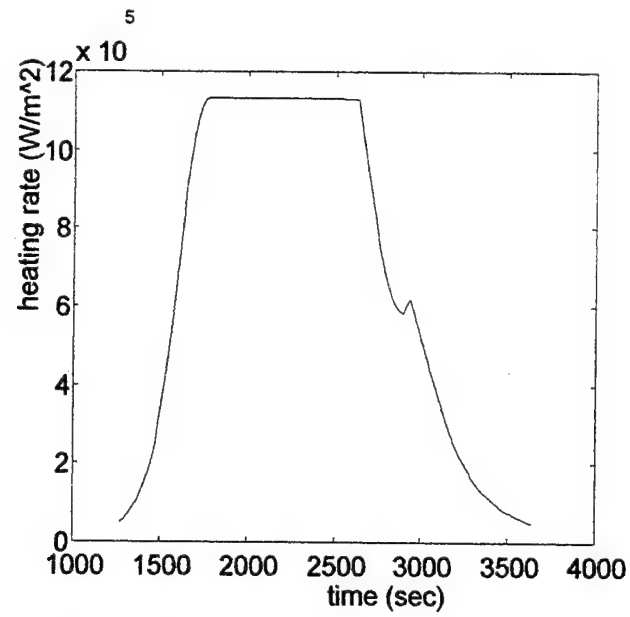


Figure 22: Heating Rate vs. Time

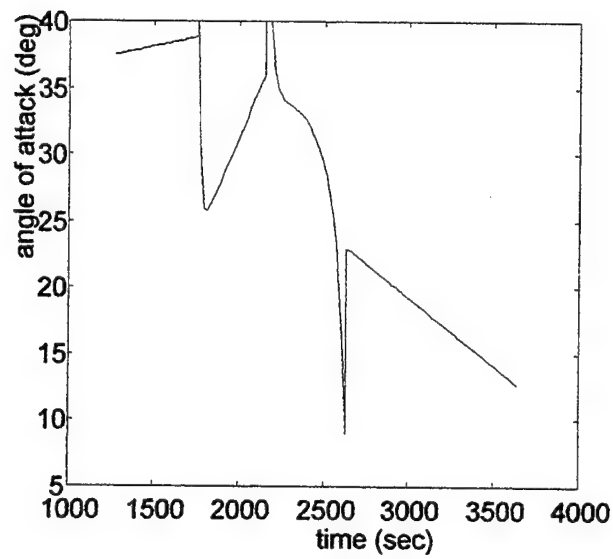


Figure 23: Angle of Attack vs. Time

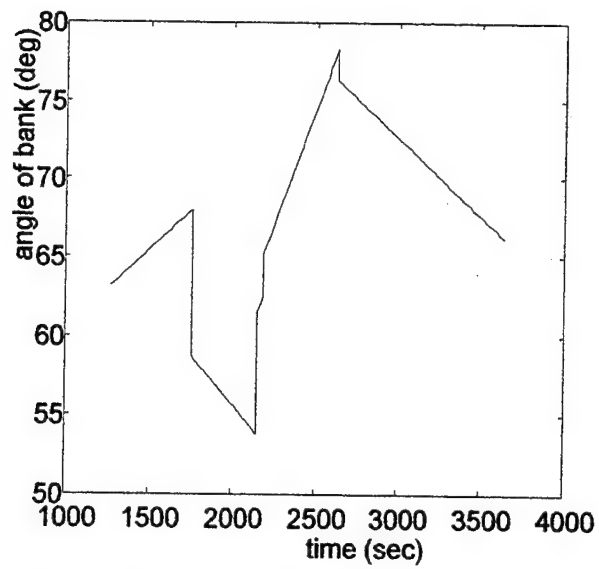


Figure 24: Angle of Bank vs. Time

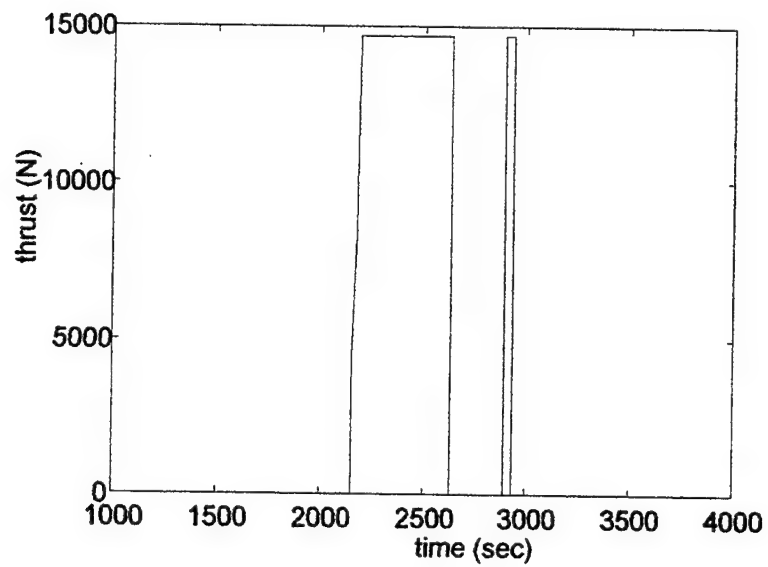


Figure 25: Thrust vs. Time



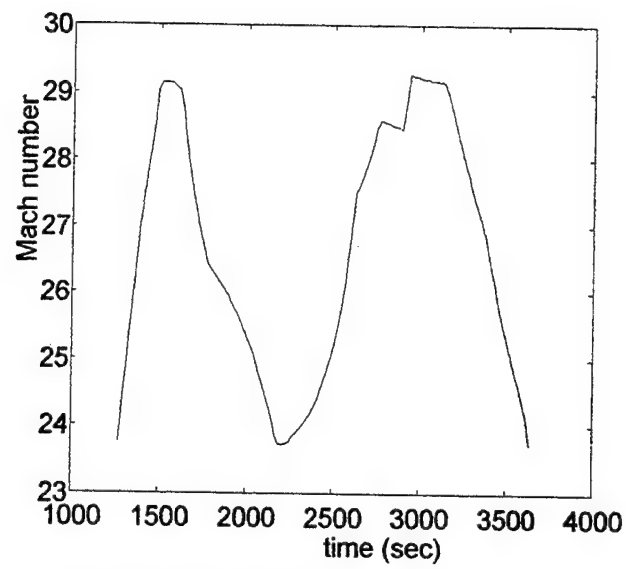


Figure 26: Mach Number vs. Time

(2) Aerocruise plots

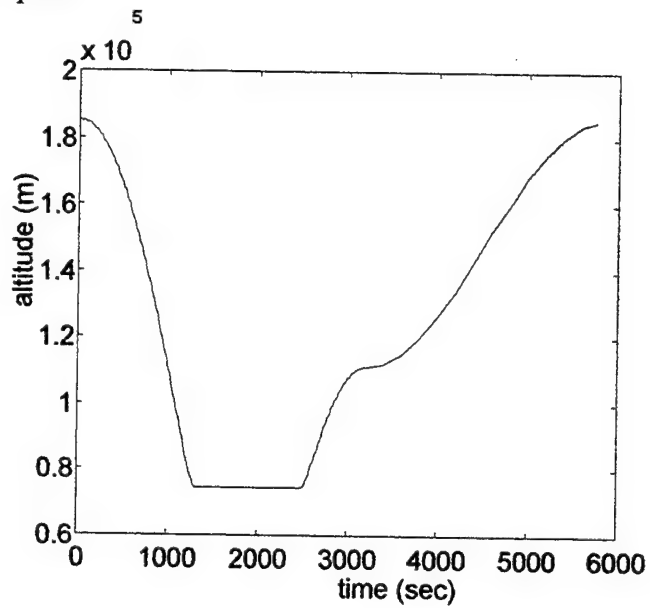


Figure 27: Altitude vs. Time

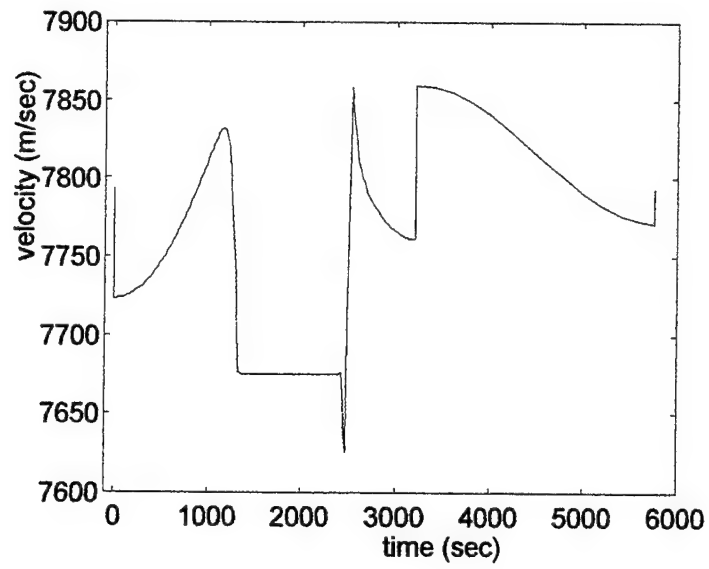


Figure 28: Velocity vs. Time

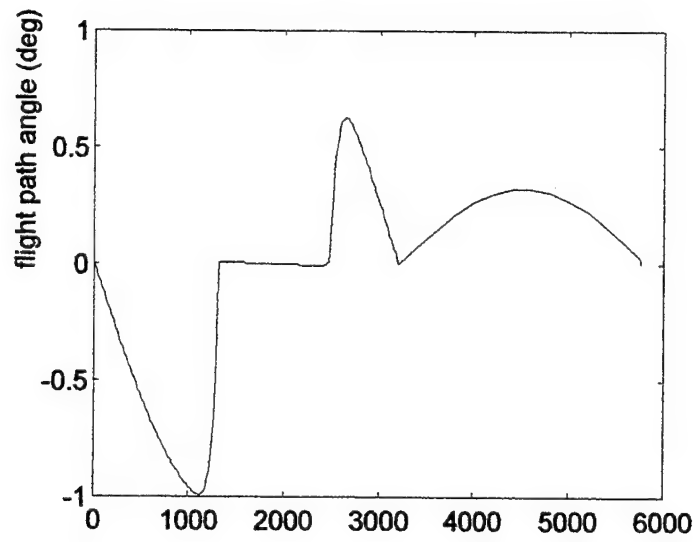


Figure 29: Flight Path Angle vs. Time

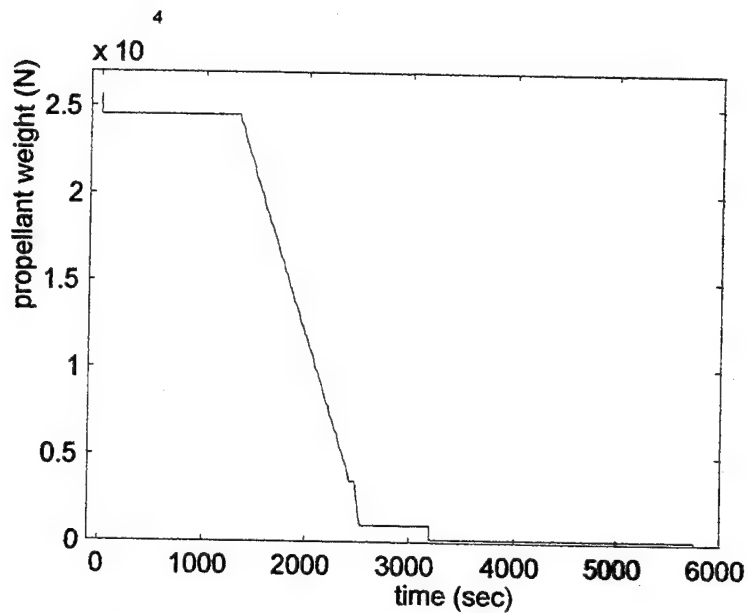


Figure 30: Propellant Weight vs. Time

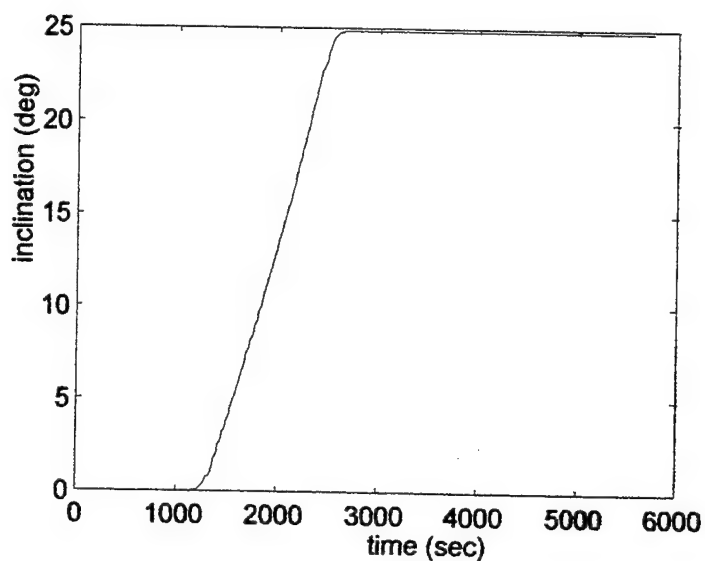


Figure 31: Inclination vs. Time

The above plots show the entire trajectory. Again, the atmosphere is only active below 111 km which corresponds, in this case, to 1271 to 3641 sec. The remaining plots will show this atmospheric pass only.

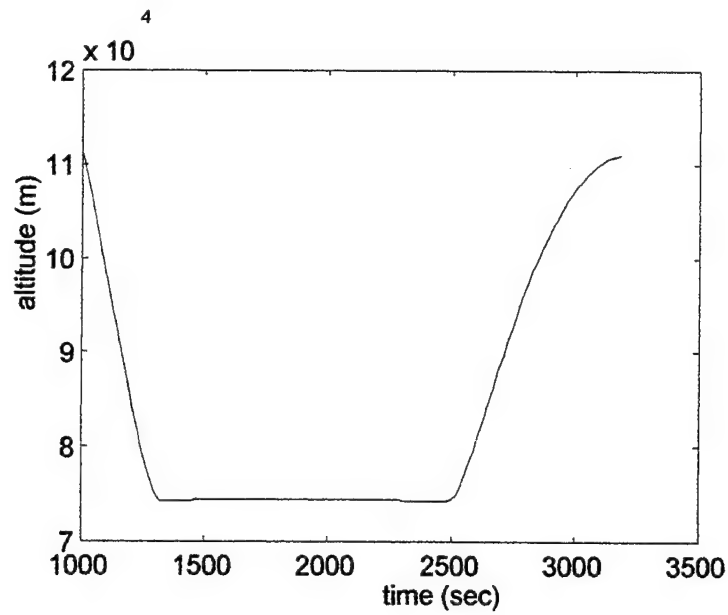


Figure 32: Altitude vs. Time

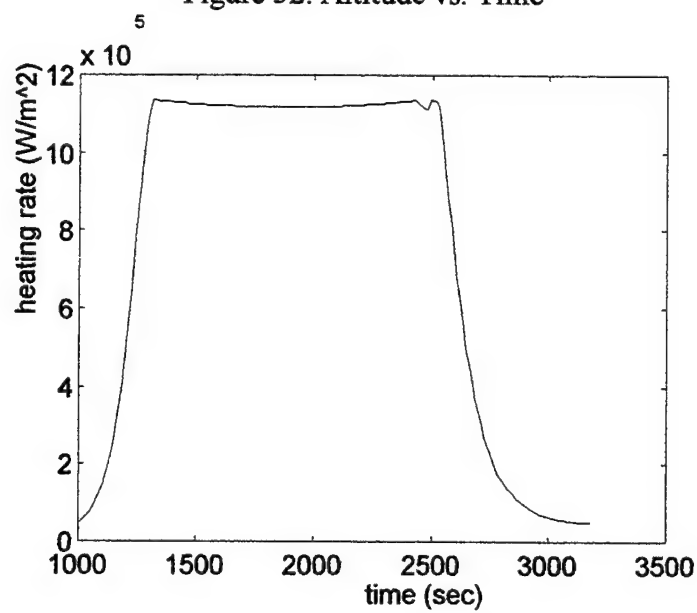


Figure 33: Heating Rate vs. Time

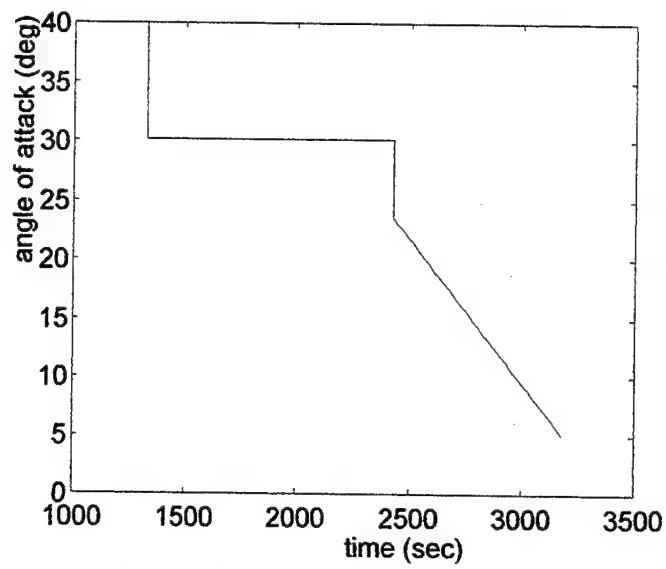


Figure 34: Angle of Attack vs. Time

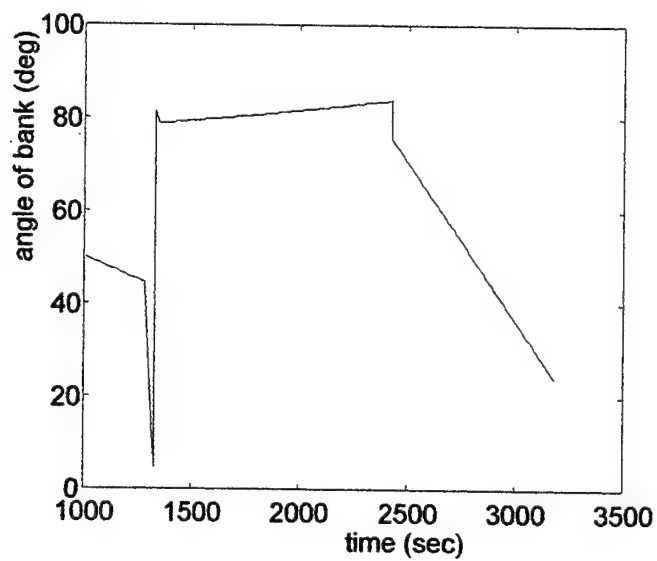


Figure 35: Angle of Bank vs. Time

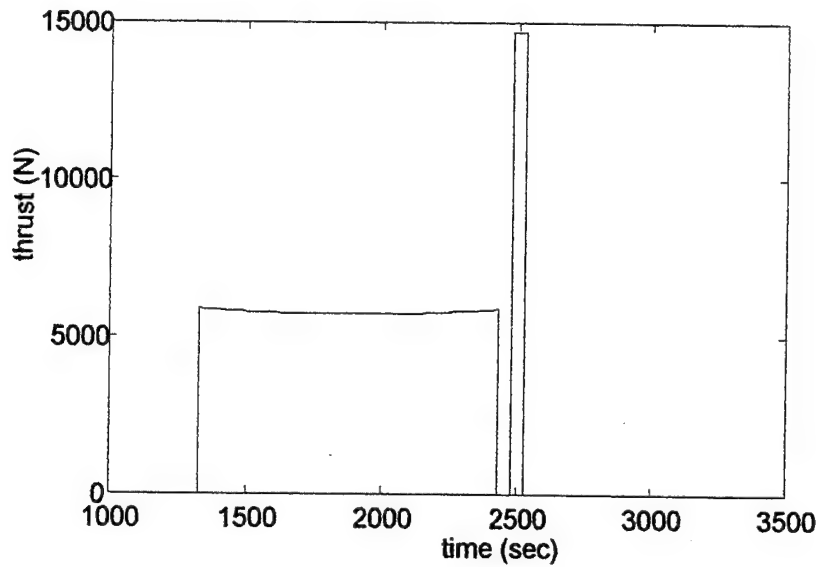


Figure 36: Thrust vs. Time

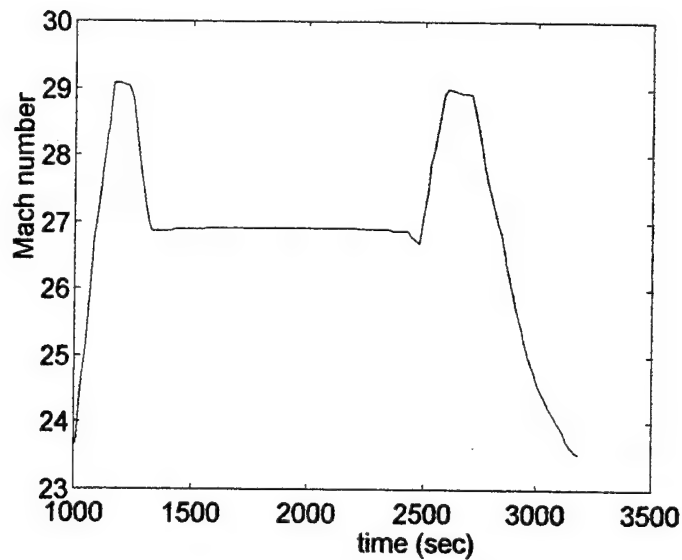


Figure 37: Mach Number vs. Time

### (3) Comparison of Results

In [Ref. 3], two trajectory characterizations were explored. The first was the previously discussed Aerocruise, and the second was called Aeroglide by the author, but is not the same as the Aeroglide previously discussed in this thesis as Aeroglide refers to an unconstrained trajectory in this thesis. The constrained arc in Aerocruise of [Ref. 3] is not among those allowed by the RMP and [Ref. 3]'s Aeroglide trajectory does not even contain a constrained arc. This is an example

where the analysis is incomplete since neither of the trajectory characterizations used satisfy the necessary conditions of the RMP.

When POST was used to optimize the Aerocruise trajectory, using the results of [Ref. 3] as a starting point, POST produced a trajectory which achieved 24.886 degrees of inclination change compared to 23.02 degrees from [Ref. 3]. The dynamics and parameterization of the problem and vehicle are identical between the two user's with one small exception. In this thesis, the skin friction term of the axial force coefficient is assumed constant for a representative altitude. This term would lead to higher drag coefficients at higher altitudes and could account for some of the performance increase. The only other difference in the analyses is in the code used. A non-linear programming code named GRG2 is used in [Ref. 3].

When POST was used to optimize the Aerobang trajectory, POST produced a trajectory which achieved 25.229 degrees of inclination change. This is only a .343 degree inclination difference but does represent at least equivalent performance if not superior performance to the Aerocruise maneuver. Again, it is not implied here that these results should prove the superiority of either maneuver. Only that a performance increase was obtained when using a characterization which was consistent with the necessary conditions of the RMP. This also shows that by using the knowledge gained from a theoretical understanding of the problem, one can influence the results in a positive way.





## V. CONCLUSIONS AND RECOMMENDATIONS

### A. CONCLUSIONS

From what has been discussed and demonstrated it is clear that whenever a user embarks on using a direct method of optimization to solve a problem, especially one as complex as the optimal aeroassisted orbital plane change, he must first ensure that he has a thorough understanding of the theoretical background of the problem. Without this knowledge, the results of any analysis will always be in question. These types of methods are very sensitive to the input given by the user and, although results will be obtained, the validity and quality of those results are most affected by the quality of the user input.

It should also be pointed out that even though this thesis could be used to support the opinion that some maneuver is superior to another, nothing in this thesis has that strength. Even if a claim of superiority could be made, no claim of optimality could be made since no attempt was made to check that all of the necessary conditions were met. This is an area of further study. Also, even if optimality had been shown here, it would only be for the MRRV from a very specific orbit into another very specific orbit, a small subset of the overall problem of designing an optimal vehicle to carry out missions which would utilize this type of maneuver.

The theory and numerical analysis performed in this thesis represent a good portion of what needs to be understood when analyzing this type of problem. It should also be noted that the theory is applicable to any atmospheric trajectory optimization with a heating rate constraint. It also offers some questions like "How can two vastly different trajectory characterizations have so close a final result?", "Does this mean that the optimal change is close to that value?", and "What would change in the results if the heating rate limit were increased or decreased?"

It is clear from the results of the numerical analysis that there is great potential in this type of maneuver for fuel and mass savings as well as pure mission flexibility in the design of future spacecraft. The best trajectory found in this thesis results in a 32% fuel

savings over the purely exoatmospheric maneuver. This problem offers such benefits that it must continue to be studied.

## **B. RECOMMENDATIONS FOR FURTHER STUDY**

The direct extension of this work which is recommended is to use the direct method to generate a "guess" to be used in the solution to the TPBVP. That algorithm could then be incorporated into a parameter optimization problem to solve definitively this optimal control problem. The initial guess needed for the TPBVP solution is in the form of the initial value for each of the costates. Seywald discusses a method of costate estimation in [Ref. 15] which shows great promise in this area. This is also an area, however, where in depth knowledge of the theoretical underpinnings of the problem is a must. Note that the discussion in [Ref. 15] uses a Minimum version of the RMP.

After this problem is solved the investigation would be extended to other missions. For elliptical orbits, the question comes up as to where in the orbit is best to initiate such a maneuver. Then the problem could expand into vehicle design and mission design. There is a vast amount to be learned in this area of research.

## APPENDIX A. SAMPLE POST INPUT FILE (AEROBANG)

The following file is an example of the input that the user provides to the POST program for optimizing an Aerobang trajectory. This particular file was used to optimize the heat rate control arcs with the rest of the arcs fixed from previous analysis. Tabs were inserted into this file for aligning the comments, however, POST will read tabs as errors. A sample MATLAB ® script is also included to show a method of generating the tables required in the input format for POST.

```
l$search
srchm = 5,           /accelerated projected gradient
maxitr = 30,         /max number of iterations
ipro = 0,
ioflag = 3,          /metric units in-out
opt = 1.0,           /+1 for maximization
optvar = 3hinc ,     /optimization variable, inclination
optph = 100.0,       /optimization phase
wopt = 0.03333,      /weighting factor (1/ opt var)
coneps = 89.9,       /gradient angle tolerance
c
c Control Variables
c
nindv = 8,           /number of control variables
indvr = 6hbnkpc2, 6hbnkpc1, 5hcritr ,
indph = 45, 45, 50,
u = -.0122452, 58.7064, 401.461,
pert = .0001, .0001, .0001,
c
indvr(4) = 6hbnkpc2, 6hbnkpc1, 5hcritr ,
indph(4) = 50, 50, 60,
u(4) = .03000305, 61.4429, 440.0094,
pert(4) = .0001, .0001, .0001,
c
indvr(7) = 6hbnkpc2, 6hbnkpc1,
indph(7) = 55, 55,
u(7) = .0299218, 65.1851,
pert(7) = .0001, .0001,
c Target Variables
c
ndepv = 1,           /number of target variables
c
```

# c Equality Constraints

c

```
depvr = 6hwprop ,
depval = 0,
deptl = 50,
depvh = 100,
```

c

\$

l\$gendat

```
maxtim = 200000.0, /200000 seconds
altmin = 40000.0, /40 km
prnc = 20, /print interval 20 sec
prnca = 20,
pinc = 20,
prnt(91) = 4halta, 4haltp, 3hinc, 6henergy, 5hvcirc, 4hmass,
prnt(97) = 6hgenv1, 6hgenv7, 6hgenv3, 6hrgenv,
prnt(101) = 6hxmax1, 3hdt, 6hgenv9, 5hpstop,
```

c

```
event = 10, /INITIALIZE 185 KM ORBIT
fesn = 100, /final event
title = 0h* Aerobang with 25k N of Fuel *,
npc(1) = 1, /conic calcs
npc(2) = 3, /Laplace conic integration method
npc(3) = 5, /initial position
altp = 185.0, /perigee altitude
alta = 185.0, /apogee altitude
inc = 0.0, /inclination
npc(5) = 0, /no atmosphere
npc(8) = 0, /aerodynamic coeff = none
sref = 11.7, /aero reference area
lref = 7.7, /aero reference length
npc(9) = 0, /propulsion type, no thrust
npc(15) = 1, /aeroheating rate calculations
npc(16) = 1, /spherical planet
omega = 0, /rotation rate of planet
npc(30) = 0, /vehicle weight model to be used
wtsg = 48041, /vehicle wt (N)
wpropi = 25643, /initial propellant wt (N)
iguid = 3, 0, 1, /inertial aero angles guidance
monx = 6hheatrt, /monitor variables
betarg = 4hone, /used to keep POST from calculating beta
endphs = 1,
$
l$gendat
event = 20, /DEORBIT IMPULSE
```

```

critr = 4htime ,           /start this event at t=5 sec
value = 5.0,
npc(2) = 1,               /RK-4 integrator
npc(9) = 3,               /Delta V insertion
isdvin = 1,               /Delta V input flag
dvimag = -47.07,          /magnitude of Delta V
ispv = 300.0,             /isp value
endphs = 1,
$
l$gendat
event = 40,               /TURN ON ATMOSPHERE AND DESCEND
critr = 6haltito,         /when altitude = 120km
value = 111000.0,
npc(2) = 1,               /RK-4 integrator
npc(5) = 2,               /1962 U.S. standard atmosphere
npc(8) = 2,               /aerocoeff, lift + drag in tables
npc(9) = 0,               /no thrust
npc(15) = 1,              /aeroheating on
iguid = 0, 1, 0,          /aero angles guidance, separate channels
iguid(6) = 1, 0, 1,       /bank and aoa polynomials
alppc = 37.50, .002777,
bnkpc = 63.11, .0100016,
$
l$tblmlt
$
l$tab

```

/table of drag coefficient vs. alpha

```

TABLE = 6HCDT , 1, 6HALPHA , 45,1,1,1,
0,0.0370, 2,0.0330, 4,0.0310, 6,0.0313, 8,0.0341,
10,0.0397, 12,0.0482, 14,0.0600, 16,0.0753, 18,0.0942,
20,0.1171, 22,0.1442, 24,0.1757, 26,0.2119, 28,0.2530,
30,0.2993, 32,0.3509, 34,0.4081, 36,0.4712, 38,0.5404,
40,0.6160, 42,0.6981, 44,0.7871, 46,0.8831, 48,0.9864,
50,1.0972, 52,1.2158, 54,1.3425, 56,1.4774, 58,1.6207,
60,1.7729, 62,1.9340, 64,2.1043, 66,2.2840, 68,2.4735,
70,2.6728, 72,2.8824, 74,3.1023, 76,3.3329, 78,3.5744,
80,3.8270, 82,4.0910, 84,4.3666, 86,4.6540, 88,4.9536,
ixtrp = 0, 0, 0, 0,
$
l$tab

```

/table of lift coefficient vs. alpha

```

TABLE = 6HCLT , 1, 6HALPHA , 45,1,1,1,
0,-0.0334, 2,-0.0211, 4,-0.0046, 6,0.0158, 8,0.0400,
10,0.0674, 12,0.0980, 14,0.1314, 16,0.1674, 18,0.2055,
20,0.2457, 22,0.2876, 24,0.3309, 26,0.3753, 28,0.4206,
30,0.4664, 32,0.5126, 34,0.5587, 36,0.6046, 38,0.6500,
40,0.6945, 42,0.7380, 44,0.7800, 46,0.8204, 48,0.8588,
50,0.8951, 52,0.9288, 54,0.9597, 56,0.9876, 58,1.0121,
60,1.0330, 62,1.0500, 64,1.0628, 66,1.0711, 68,1.0747,
70,1.0733, 72,1.0666, 74,1.0543, 76,1.0361, 78,1.0118,
80,0.9811, 82,0.9436, 84,0.8992, 86,0.8475, 88,0.7883,
ixtrp = 0, 0, 0, 0,
endphs = 1,
$
l$gendat
event = 45, /BEGIN ZERO THRUST HEAT CONTROL ARC
citr = 6hheatrt,
value = 11.3e+05, /100 Btu/ft^2*s
npc(8) = 2, /aero coeff fm tables
npc(9) = 1, /rocket engine
iwdf = 2, /calculate using isp and thrust
ispv = 300.0, /isp
iengmf = 0, /turn off rocket engine
npc(15) = 1, /aeroheating calcs
iguid = 0, 1, 0, /aero angles guidance
iguid(6) = 2, 0, 1, /aoa angle from tables
bnkpc = 58.7064, -.0122452,
$
l$tblmlt

```

/list of table multipliers

```

genv7m(1)= 5.85, 6hdens , / Aref/2*density
genv6m(1)= .15873 , 6hgenv9 , / .5*beta/3.15
genv4m(2)= 4hmass , / mass
genv3m(2)= 5hgenv4 , / mass*sin(gamma)
$
l$stab
table = 5htvc1t , 0, 14679.0,
$
l$stab
table = 6halphat, 2, 5hgenv3 , 5hgenv7 , 81, 96, 1,1,1,1,1,1,1,1,

```

This was a bivariant table which took genv3 and genv7 and output the required alpha. This is the solution to  $p=0$  for the case of  $T=0$ . See the MATLAB ® script for now to generate this type of table.

```
ixtrp = 0,0,0,0,
$
l$tab
```

```

                                     /table for v^2 multiplied above by  $\xi$ 
table = 6hgenv3t, 1, 5hgenv5, 2, 1, 1, 1,
-10000.0,-10000.0,10000.0,10000.0,
$
l$tab
```

```

                                     /table of sin(gamma) multiplied above by mass
table = 6hgenv4t, 1, 6hgammaa, 13, 1, 1, 1,
-10.0000, -0.17365, -8.0000, -0.13917, -6.0000, -0.10453,
-4.0000, -0.06976, -2.0000, -0.03490, -0.5000, -0.0087,
0.0000, 0.00000, 0.5000, 0.0087, 2.0000, 0.03490,
4.0000, 0.06976, 6.0000, 0.10453, 8.0000, 0.13917,
10.0000, 0.17365,
$
l$tab
```

```

                                     /table of atmospheric  $\beta$  taken from 1962 data. This was
                                     /done by simulating a trajectory the crashed to the ground
                                     /using MATLAB ® to convert altitude and density to  $\beta$ .
table = 6hgenv9t, 1, 6haltito, 58, 1, -1, 1,
110120, 1.55e-04, 108333, 1.51e-04, 106523, 1.56e-04, 104715, 1.63e-04,
102910, 1.69e-04, 101111, 1.76e-04, 99319, 1.74e-04, 97535, 1.78e-04,
95762, 1.83e-04, 94002, 1.88e-04, 92257, 1.93e-04, 90531, 1.95e-04,
88828, 1.84e-04, 87154, 1.84e-04, 85515, 1.84e-04, 83919, 1.84e-04,
82374, 1.84e-04, 80893, 1.84e-04, 79489, 1.64e-04, 78175, 1.57e-04,
76965, 1.53e-04, 75870, 1.50e-04, 74901, 1.47e-04, 74065, 1.45e-04,
73366, 1.43e-04, 72804, 1.41e-04, 72374, 1.40e-04, 72067, 1.39e-04,
71869, 1.39e-04, 71764, 1.39e-04, 71731, 1.39e-04, 71750, 1.39e-04,
71797, 1.39e-04, 71852, 1.39e-04, 71892, 1.39e-04, 71898, 1.39e-04,
71851, 1.39e-04, 71736, 1.39e-04, 71537, 1.38e-04, 71242, 1.37e-04,
70952, 1.37e-04, 70661, 1.36e-04, 70359, 1.35e-04, 70119, 1.35e-04,
69891, 1.34e-04, 69650, 1.34e-04, 69384, 1.33e-04, 69089, 1.32e-04,
68758, 1.31e-04, 68440, 1.31e-04, 68132, 1.30e-04, 67842, 1.29e-04,
67623, 1.29e-04, 67459, 1.29e-04, 67336, 1.28e-04, 67250, 1.28e-04,
67201, 1.28e-04, 67190, 1.28e-04,
$
l$tab
```

```

                                     /table of  $\mu/(R_{earth}+altito)^2+genv6$ 
table = 6hgenv5t, 2, 6hgenv6, 6haltito, 12, 7,
```

```

1, 1, 1, 1, 1, 1, 1, 1,
50000,
400, 409.65, 600, 609.65, 800, 809.65, 1000, 1009.65,
1200, 1209.65, 1400, 1409.65, 1600, 1609.65, 1800, 1809.65,
2000, 2009.65, 2200, 2209.65, 2400, 2409.65, 2600, 2609.65,
60000,
400, 409.62, 600, 609.62, 800, 809.62, 1000, 1009.62,
1200, 1209.62, 1400, 1409.62, 1600, 1609.62, 1800, 1809.62,
2000, 2009.62, 2200, 2209.62, 2400, 2409.62, 2600, 2609.62,
70000,
400, 409.59, 600, 609.59, 800, 809.59, 1000, 1009.59,
1200, 1209.59, 1400, 1409.59, 1600, 1609.59, 1800, 1809.59,
2000, 2009.59, 2200, 2209.59, 2400, 2409.59, 2600, 2609.59,
80000,
400, 409.56, 600, 609.56, 800, 809.56, 1000, 1009.56,
1200, 1209.56, 1400, 1409.56, 1600, 1609.56, 1800, 1809.56,
2000, 2009.56, 2200, 2209.56, 2400, 2409.56, 2600, 2609.56,
90000,
400, 409.53, 600, 609.53, 800, 809.53, 1000, 1009.53,
1200, 1209.53, 1400, 1409.53, 1600, 1609.53, 1800, 1809.53,
2000, 2009.53, 2200, 2209.53, 2400, 2409.53, 2600, 2609.53,
100000,
400, 409.50, 600, 609.50, 800, 809.50, 1000, 1009.50,
1200, 1209.50, 1400, 1409.50, 1600, 1609.50, 1800, 1809.50,
2000, 2009.50, 2200, 2209.50, 2400, 2409.50, 2600, 2609.50,
110000,
400, 409.47, 600, 609.47, 800, 809.47, 1000, 1009.47,
1200, 1209.47, 1400, 1409.47, 1600, 1609.47, 1800, 1809.47,
2000, 2009.47, 2200, 2209.47, 2400, 2409.47, 2600, 2609.47,
$
l$tab

```

/table of  $v^2$  multiplied above by  $\xi$

```

table = 6hgenv6t, 1, 4hvela, 6, 1, 1, 1,
5000.0000, 25000000.000, 6000.0000, 36000000.000,
6500.0000, 42250000.000, 7000.0000, 49000000.000,
7500.0000, 56250000.000, 8000.0000, 64000000.000,
$
l$tab

```

/table of  $v^2$  multiplied above by  $\frac{1}{2} \cdot \rho \cdot A_{ref}$

```

table = 6hgenv7t, 1, 4hvela, 6, 1, 1, 1,
5000.0000, 25000000.000, 6000.0000, 36000000.000,
6500.0000, 42250000.000, 7000.0000, 49000000.000,
7500.0000, 56250000.000, 8000.0000, 64000000.000,

```



```

endphs = 1,
$
l$gendat
event = 50, /BEGIN MAX AOA TRANSITION ARC
critr = 6htdurp, /begin after a certain time period.
value = 401.461,
npc(8) = 2, /aero coeff fm tables
npc(9) = 1, /rocket engine
npc(22) = 3, /throttling paramter from table
iwdf = 2, /calculate using isp and thrust
ispv = 300.0, /isp
iengmf = 1, /turn on rocket engine
npc(15) = 1, /aeroheating calcs
iguid = 0, 1, 0, /aero angles guidance
iguid(6) = 1, 0, 1,
alppc = 40,0,0,0, / max aoa
bnkpc = 61.4429, .03000305,
$
l$tblmlt
genv7m(1)= 5.85, 6hdens ,
genv6m(1)= .15873 , 6hgenv9 ,
genv4m(2)= 4hmass ,
genv3m(2)= 5hgenv4 ,
etam = 8.893026e-5, /1/Tmax to convert required thrust to throttling
/parameter
$
l$stab
table = 5htvc1t , 0, 14679.0,
$
l$stab

/table of thrust=drag+genv3
table = 6hetat , 2, 6hdrag , 6hgenv3 , 2, 2, 1, 1, 1, 1, 1, 1, 1, 1,
-100000,
-100000, -200000, 100000, 0,
100000,
-100000, 0, 100000, 200000,
ixtrp = 0,0,0,0,
$
l$stab

/table of genv5 multiplied above by genv4
table = 6hgenv3t, 1, 5hgenv5, 2, 1, 1, 1,
-10000.0,-10000.0,10000.0,10000.0,
$

```

l\$tab

/table of sin(gamma) multiplied above by mass

```
table = 6hgenv4t, 1, 6hgammaa, 13, 1, 1, 1,  
-10.0000, -0.17365, -8.0000, -0.13917, -6.0000, -0.10453,  
-4.0000, -0.06976, -2.0000, -0.03490, -0.5000, -0.0087,  
0.0000, 0.00000, 0.5000, 0.0087, 2.0000, 0.03490,  
4.0000, 0.06976, 6.0000, 0.10453, 8.0000, 0.13917,  
10.0000, 0.17365,  
$
```

l\$tab

/ see genv9 table previous phase

```
table = 6hgenv9t, 1, 6haltito, 58, 1, -1, 1,  
110120, 1.55e-04, 108333, 1.51e-04, 106523, 1.56e-04, 104715, 1.63e-04,  
102910, 1.69e-04, 101111, 1.76e-04, 99319, 1.74e-04, 97535, 1.78e-04,  
95762, 1.83e-04, 94002, 1.88e-04, 92257, 1.93e-04, 90531, 1.95e-04,  
88828, 1.84e-04, 87154, 1.84e-04, 85515, 1.84e-04, 83919, 1.84e-04,  
82374, 1.84e-04, 80893, 1.84e-04, 79489, 1.64e-04, 78175, 1.57e-04,  
76965, 1.53e-04, 75870, 1.50e-04, 74901, 1.47e-04, 74065, 1.45e-04,  
73366, 1.43e-04, 72804, 1.41e-04, 72374, 1.40e-04, 72067, 1.39e-04,  
71869, 1.39e-04, 71764, 1.39e-04, 71731, 1.39e-04, 71750, 1.39e-04,  
71797, 1.39e-04, 71852, 1.39e-04, 71892, 1.39e-04, 71898, 1.39e-04,  
71851, 1.39e-04, 71736, 1.39e-04, 71537, 1.38e-04, 71242, 1.37e-04,  
70952, 1.37e-04, 70661, 1.36e-04, 70359, 1.35e-04, 70119, 1.35e-04,  
69891, 1.34e-04, 69650, 1.34e-04, 69384, 1.33e-04, 69089, 1.32e-04,  
68758, 1.31e-04, 68440, 1.31e-04, 68132, 1.30e-04, 67842, 1.29e-04,  
67623, 1.29e-04, 67459, 1.29e-04, 67336, 1.28e-04, 67250, 1.28e-04,  
67201, 1.28e-04, 67190, 1.28e-04,  
$
```

l\$tab

/see genv5 table previous phase

```
table = 6hgenv5t, 2, 6hgenv6, 6haltito, 12, 7,  
1, 1, 1, 1, 1, 1, 1, 1,  
50000,  
400, 409.65, 600, 609.65, 800, 809.65, 1000, 1009.65,  
1200, 1209.65, 1400, 1409.65, 1600, 1609.65, 1800, 1809.65,  
2000, 2009.65, 2200, 2209.65, 2400, 2409.65, 2600, 2609.65,  
60000,  
400, 409.62, 600, 609.62, 800, 809.62, 1000, 1009.62,  
1200, 1209.62, 1400, 1409.62, 1600, 1609.62, 1800, 1809.62,  
2000, 2009.62, 2200, 2209.62, 2400, 2409.62, 2600, 2609.62,  
70000,  
400, 409.59, 600, 609.59, 800, 809.59, 1000, 1009.59,
```

```

1200, 1209.59, 1400, 1409.59, 1600, 1609.59, 1800, 1809.59,
2000, 2009.59, 2200, 2209.59, 2400, 2409.59, 2600, 2609.59,
80000,
400, 409.56, 600, 609.56, 800, 809.56, 1000, 1009.56,
1200, 1209.56, 1400, 1409.56, 1600, 1609.56, 1800, 1809.56,
2000, 2009.56, 2200, 2209.56, 2400, 2409.56, 2600, 2609.56,
90000,
400, 409.53, 600, 609.53, 800, 809.53, 1000, 1009.53,
1200, 1209.53, 1400, 1409.53, 1600, 1609.53, 1800, 1809.53,
2000, 2009.53, 2200, 2209.53, 2400, 2409.53, 2600, 2609.53,
100000,
400, 409.50, 600, 609.50, 800, 809.50, 1000, 1009.50,
1200, 1209.50, 1400, 1409.50, 1600, 1609.50, 1800, 1809.50,
2000, 2009.50, 2200, 2209.50, 2400, 2409.50, 2600, 2609.50,
110000,
400, 409.47, 600, 609.47, 800, 809.47, 1000, 1009.47,
1200, 1209.47, 1400, 1409.47, 1600, 1609.47, 1800, 1809.47,
2000, 2009.47, 2200, 2209.47, 2400, 2409.47, 2600, 2609.47,
$
l$tab

```

```

                                     /see previous phase
table = 6hgenv6t, 1, 4hvela, 6, 1, 1, 1,
5000.0000, 25000000.000, 6000.0000, 36000000.000,
6500.0000, 42250000.000, 7000.0000, 49000000.000,
7500.0000, 56250000.000, 8000.0000, 64000000.000,
$
l$tab

```

```

                                     /see previous phase
table = 6hgenv7t, 1, 4hvela, 6, 1, 1, 1,
5000.0000, 25000000.000, 6000.0000, 36000000.000,
6500.0000, 42250000.000, 7000.0000, 49000000.000,
7500.0000, 56250000.000, 8000.0000, 64000000.000,
endphs = 1,
$
l$gendat
event = 55, /BEGIN MAX THRUST ARC
critr = 6heta, /begin when thrust reaches max
value = 1,
npc(22) = 0,
npc(8) = 2, /aero coeff fm tables
npc(9) = 1, /rocket engine
iwdf = 2, /calculate using isp and thrust
ispv = 300.0, /isp

```

```

iengmf = 1,          /turn on rocket engine
npc(15) = 1,         /aeroheating calcs
iguid = 0, 1, 0,     /aero angles guidance
iguid(6) = 2, 0, 1,  /aoa angle from tables
bnkpc = 65.1851, .0299218,
$
l$tblmlt
genv7m(1)= 5.85, 6hdens ,
genv6m(1)= .15873 , 6hgenv9 ,
genv4m(2)= 4hmass ,
genv3m(2)= 5hgenv4 ,
$
l$tab
table = 5htvc1t , 0, 14679.0,
$
l$tab
table = 6halphat, 2, 5hgenv3 , 5hgenv7 , 111, 96, 1,1,1,1,1,1,1,

```

alpha table as in phase 45 but solution of p=0 for T=Tmax

```

ixtrp = 0,0,0,0,
endphs = 1,
$
l$gendat
event = 60,          /Ascend to top of atmosphere
critr = 6htdurp ,
value = 440.0094,
npc(8) = 2,          /aero coeff in tables
npc(9) = 1,          /rocket engine
iwdf = 2,            /calculate using isp and thrust
ispv = 300.0,        /isp
iengmf = 0,          /turn off rocket engine
npc(15) = 1,         /aeroheating
iguid = 0, 1, 0,     /aero angles guidance
iguid(6) = 1, 0, 1,
bnkpc = 76.28, -.010020, /
alppc = 22.96, -.01019,
bnkarg = 6htdurp ,   /used here so bank angle is continuous through events 60.1
                        /and 60.2
alparg = 6htdurp ,   /same as bank angle
$
l$tblmlt
$
l$tab
table = 5htvc1t , 0, 14679.0,

```

```

endphs = 1,
$
l$gendat
event = 60.1,           /thrust if needed
critr = 6hgammai,      /if don't get to 111 km then thrust at apogee
value = 0,
npc(8) = 2,            /aero coeff in tables
npc(9) = 1,            /rocket engine
iwdf = 2,              /calculate using isp and thrust
ispv = 300.0,          /isp
iengmf = 1,            /turn on rocket engine
npc(15) = 1,           /aeroheating
iguid = 0, 1, 0,       /aero angles guidance
iguid(6) = 1, 0, 1,
$
l$tblmlt
$
l$stab
table = 5htvc1t, 0, 14679.0,
endphs = 1,
$
l$gendat
event = 60.2,           /thrust if needed
critr = 6halta,        /if don't get to 111 km then thrust at apogee
value = 185.0,
npc(8) = 2,            /aero coeff in tables
npc(9) = 1,            /rocket engine
iwdf = 2,              /calculate using isp and thrust
ispv = 300.0,          /isp
iengmf = 0,            /turn off rocket engine
npc(15) = 1,           /aeroheating
iguid = 0, 1, 0,       /aero angles guidance
iguid(6) = 1, 0, 1,
$
l$tblmlt
$
l$stab
table = 5htvc1t, 0, 14679.0,
endphs = 1,
$
l$gendat
event = 80,             /EXIT ATMOSPHERE
critr = 6haltito,
value = 111000.0,
npc(5) = 0,            /no atmosphere

```

```

npc(8) = 0, /no aero coeff
iengmf = 0, /turn off rocket engine
iguid = 0, 1, 0, /aero angles guidance
iguid(6) = 1, 1, 1,
banki = 0,
alphi = 0,
betai = 0,
betpc = 0, 0, 0, 0,
alppc = 0, 0, 0, 0,
bnkpc = 0, 0, 0, 0,
endphs = 1,
$
l$gendat
event = 80.1, /START REORBIT IMPULSE
critr = 6hgammai, /Start the reorbit impulse if gamma=0
value = 0,
npc(9) = 1, /rocket engine
npc(5) = 0, /no atmosphere
npc(8) = 0, /no aero coeff
iwdf = 2, /calculate using isp and thrust
ispv = 300,
iengmf = 1, /turn on rocket engine
$
l$tblmlt
$
l$tab
table = 5htvc1t, 0, 1500000.0, /1000 times normal max thrust
endphs = 1,
$
l$gendat
event = 80.2, /END REORBIT IMPULSE
critr = 6halta, /stop the impulse when apogee=185km
value = 185.1,
npc(2) = 3, /Laplace conic integration method
dt = 100,
prnc = 200, /print interval 200 sec
prnca = 200,
pinc = 200,
npc(5) = 0, /no atmosphere
npc(8) = 0, /no aero coeff
iengmf = 0, /turn off rocket engine
iwdf = 2, /calculate using isp and thrust
$
l$tblmlt
$

```

```

l$tab
table = 5htvc1t, 0, 1500000.0,
endphs = 1,
$
l$gendat
event = 90, /CIRCULARIZATION IMPULSE
critr = 6haltito,
value = 185000.0,
npc(9) = 3,
ispv = 300,
isdvin = 0.0,
endphs = 1,
$
l$gendat
event = 100, /END RUN
critr = 6htdurp,
value = 5.0,
endphs = 1,
endprb = 1,
endjob = 1,
$

```

The following is an example of a MATLAB ® script used to generate some of the tables

```

% compute the tables needed for the heat rate control portion
% of the orbit. Makes a function of required angle of attack for the max thrust arc.
% this file was named MRRVTtab.m and executed at the MATLAB ® command line

```

```

a=0;
for gv7=5000:1000:100000,
    a=a+1;
    b=0;
    for gv3=-80000:1000:30000,
        b=b+1;
        pol=[-gv7*4.9852e-6 -14679*.48907*(pi/180)^2-gv7*2.2429e-4 -
14679*.00305*pi/180+gv7*2.4732e-3 14679*1.0024-gv7*3.6994e-2-gv3];

% the above polynomial is for the solution of p=0 for max thrust as a function of genv7
% and genv3.

    alphaposs=roots(pol);
% the possible alpha's are the roots of the polynomial
% the below if/then structure finds the real root.
    if (imag(alphaposs(1))==0 & imag(alphaposs(2))==0 & imag(alphaposs(3))==0)
        alpha1=max(alphaposs);
    end
end
end

```

```

else
    for x=1:3,
        if imag(alphaposs(x))==0
            alpha1=alphaposs(x);
        end
    end
end
if alpha1<0    % if the real root is negative 0 is substituted this reduces
               % interpolation errors
    alpha1=0;
end
alpha(a,b)=alpha1;
end
end
fid=fopen('MRRVTtable','w');                % opens a file for the output
a=0;

% This section creates the table using formatted output to above file 3 columns of pairs
for gv7=5000:1000:100000,
    a=a+1;
    b=-2;
    fprintf(fid,'%8.0f\n',[gv7]);
    for gv3=-80000:3000:30000,
        b=b+3;
        for p=0:1,
            fprintf(fid,'%9.0f,%5.2f',[gv3+p*1000 alpha(a,b+p)]);
        end
        fprintf(fid,'%9.0f,%5.2f\n',[gv3+2000 alpha(a,b+2)]);
    end
end
end

```



## APPENDIX B. SAMPLE POST INPUT FILE (AEROCRUISE)

The following file is an example of the input that the user provides to the POST program for optimizing an Aerocruise trajectory. This particular file was used to optimize the heat rate control, and atmospheric exit arcs with the rest of the arcs fixed from previous analysis. Tabs were inserted into this file for aligning the comments, however, POST will read tabs as errors.

l\$search

c

```
srchm = 5,           /activate optimization feature
maxitr = 30,         /max number of iterations
ipro = 0,           /
ioflag = 3,         /metric units in-out
opt = 1.0,          /+1 for maximization
optvar = 6hinc,      /optimization variable, inclination
optph = 100.0,      /optimization phase
wopt = 0.04,        /weighting factor (1/ opt var)
coneps = 89.9,
```

c

```
nindv = 6,           /number of control var
indvr = 6halppc2, 6hbnkpc2,
indph = 60, 60,
u = 0, -.07,
pert = .0001, .0001,
```

c

```
indvr(3) = 6hcritr, 6halppc1, 6halppc1, 6hbnkpc1,
indph(3) = 60, 60, 50, 60,
u(3) = 1115.2, 40, 29.329, 60,
pert(3) = .0001, .0001, .0001, .0001,
```

c

c Equality Constraints

c

```
ndepv = 5,           /number of target var
depvr = 6hwprop,
depval = 0.0,
dephi = 50,
depph = 100.0,
```

c

c Inequality Constraints

/ these inequality constraints in POST are evaluated at the  
/termination of the pervious phase to the one listed for the

/constraint. This poses an interesting problem in using them to  
 /ensure a limit is not violated during the duration of a phase and

not

/just at the end.

c

depvr(2) = 6hheatrt, 6hheatrt, 6hheatrt, 6halpha,  
 depval(2) = 1.135e+06, 1.13e+06, 1.13e+06, 5,  
 depvh(2) = 60, 60.1, 60.2, 80,  
 idepvr(2) = 1, 1, 1, -1,

c

\$

l\$gendat

maxtim = 20000.0, /20000 seconds  
 altmin = 40000.0, /40 km  
 prnca = 20.0,  
 pinc = 20.0,  
 prnc = 20,  
 prnt(91) = 4halta, 4haltp, 3hinc, 6henergy, 5hvcirc, 4hmass,  
 prnt(97) = 6hgenv1, 6hgenv2, 6hgenv3, 6hrgenv,  
 prnt(101) = 6hxmax1, 5hpstop,

c

event = 10, /INITIALIZE 185 KM ORBIT  
 fesn = 100,  
 title = 0h\* Aerocruise with 25k N of Fuel \*,

c

npc(1) = 1, /conic calcs  
 npc(2) = 3, /Laplace conic integration method  
 npc(3) = 5, /initial position  
 altp = 185.0,  
 alta = 185.0,  
 inc = 0.0,  
 npc(5) = 0, /no atmosphere  
 npc(8) = 0, /aerodynamic coeff = none  
 sref = 11.7, /aero reference area  
 npc(9) = 0, /propulsion type, no thrust  
 npc(15) = 1, /aeroheating rate calculations  
 npc(16) = 1, /spherical planet  
 omega = 0, /rotation rate of planet  
 npc(30) = 0, /vehicle weight model to be used  
 wgtsg = 48041, /vehicle wt (N)  
 wpropi = 25643, /initial propellant wt (N)  
 iguid = 3, 0, 1, /inertial aero angles guidance  
 monx = 6hheatrt, /monitor variables  
 betarg = 4hone,  
 endphs = 1,

```

$
l$gendat
event = 20,           /DEORBIT IMPULSE
critr = 4htime,
value = 5.0,
npc(2) = 1,           /RK-4 integrator
npc(9) = 3,           /Delta V insertion
isdvin = 1,           /Delta V input flag
dvimag = -70.2,       /magnitude of the Delta V
ispv = 300.0,         /isp value
endphs = 1,
$
l$gendat
event = 40,           /TURN ON ATMOSPHERE & DESCEND
critr = 6haltito,
value = 111000.0,
npc(2) = 1,           /RK-4 integrator
npc(5) = 2,           /1962 standard atmosphere
npc(8) = 2,           /aerocoeff, lift + drag in tables
npc(9) = 0,           /no thrust
npc(15) = 1,          /aeroheating on
iguid = 0, 1, 0,      /aero angles guidance, separate channels
iguid(6) = 1, 0, 1,   /bank and aoa polynomials
alppc = 40, 0,
bnkpc = 50, -.02,
$
l$tblmlt
$
l$stab
                                     /table of drag coefficient vs alpha
TABLE = 6HCDT , 1, 6HALPHA , 45,1,1,1,
0,0.0370, 2,0.0330, 4,0.0310, 6,0.0313, 8,0.0341,
10,0.0397, 12,0.0482, 14,0.0600, 16,0.0753, 18,0.0942,
20,0.1171, 22,0.1442, 24,0.1757, 26,0.2119, 28,0.2530,
30,0.2993, 32,0.3509, 34,0.4081, 36,0.4712, 38,0.5404,
40,0.6160, 42,0.6981, 44,0.7871, 46,0.8831, 48,0.9864,
50,1.0972, 52,1.2158, 54,1.3425, 56,1.4774, 58,1.6207,
60,1.7729, 62,1.9340, 64,2.1043, 66,2.2840, 68,2.4735,
70,2.6728, 72,2.8824, 74,3.1023, 76,3.3329, 78,3.5744,
80,3.8270, 82,4.0910, 84,4.3666, 86,4.6540, 88,4.9536,
ixtrp = 0, 0, 0, 0,
$
l$stab
                                     /table of lift coefficient vs alpha

```

```

TABLE = 6HCLT , 1, 6HALPHA , 45,1,1,1,
0,-0.0334, 2,-0.0211, 4,-0.0046, 6,0.0158, 8,0.0400,
10,0.0674, 12,0.0980, 14,0.1314, 16,0.1674, 18,0.2055,
20,0.2457, 22,0.2876, 24,0.3309, 26,0.3753, 28,0.4206,
30,0.4664, 32,0.5126, 34,0.5587, 36,0.6046, 38,0.6500,
40,0.6945, 42,0.7380, 44,0.7800, 46,0.8204, 48,0.8588,
50,0.8951, 52,0.9288, 54,0.9597, 56,0.9876, 58,1.0121,
60,1.0330, 62,1.0500, 64,1.0628, 66,1.0711, 68,1.0747,
70,1.0733, 72,1.0666, 74,1.0543, 76,1.0361, 78,1.0118,
80,0.9811, 82,0.9436, 84,0.8992, 86,0.8475, 88,0.7883,
ixtrp = 0, 0, 0, 0,
endphs = 1,
$
l$gendat
event = 45, /make gamma go to zero
critr = 6hheatrt,
value = 1.00e+06, /this value chosen by trial and error to get heat rate at
/gamma=0 to be max allowed

npc(8) = 2, /aero coeff fm tables
npc(9) = 1, /rocket engine
iwdf = 2, /calculate using isp and thrust
ispv = 300.0, /isp
iengmf = 1, /turn on rocket engine
npc(15) = 1, /aeroheating calcs
iguid = 0, 1, 0, /aero angles guidance
iguid(6) = 1, 0, 0,
bnkpc(2) = -.80,
alppc = 40,0,0,0,
endphs = 1,
$
l$gendat
event = 50, /BEGIN AEROCRUISE ARC
critr = 6hgammai ,
value = .006, /level flight
npc(8) = 2, /aero coeff fm tables
npc(9) = 1, /rocket engine
iwdf = 2, /calculate using isp and thrust
ispv = 300.0, /isp
iengmf = 1, /turn on rocket engine
npc(15) = 1, /aeroheating calcs
npc(22) = 3, /throttling parameter from table
iguid = 0, 1, 0, /aero angles guidance
iguid(6) = 1, 0, 2, /bank angle from tables
$
l$tblmlt

```

```

genv2m(2) = 6hgenv4 ,
genv3m(2) = 6hthrust ,
genv4m(2) = 4hmass,
etam      = 6.812453e-05, 6hdrag ,
$
l$tab

```

```

                                /table of lift+genv3
table = 6hgenv1t, 2, 6hlift , 6hgenv3 , 2, 2, 1, 1, 1, 1, 1, 1, 1, 1,
-100000,
-100000, -200000, 100000, 0,
100000,
-100000, 0, 100000, 200000,
ixtrp = 0,0,0,0,
$
l$tab

```

```

                                /table of cos(gamma) multiplied above by genv4
table = 6hgenv2t, 0, 1,
$
l$tab

```

```

                                /table of sin(alpha) multiplied above by thrust
table = 6hgenv3t, 1, 6halpha ,44, 1, 1, 1,
0,0.00000, 1,0.01745, 2,0.03490, 3,0.05234,
4,0.06976, 5,0.08716, 6,0.10453, 7,0.12187,
8,0.13917, 9,0.15643, 10,0.17365, 11,0.19081,
12,0.20791, 13,0.22495, 14,0.24192, 15,0.25882,
16,0.27564, 17,0.29237, 18,0.30902, 19,0.32557,
20,0.34202, 21,0.35837, 22,0.37461, 23,0.39073,
24,0.40674, 25,0.42262, 26,0.43837, 27,0.45399,
28,0.46947, 29,0.48481, 30,0.50000, 31,0.51504,
32,0.52992, 33,0.54464, 34,0.55919, 35,0.57358,
36,0.58779, 37,0.60182, 38,0.61566, 39,0.62932,
40,0.64279, 41,0.65606, 42,0.66913, 43,0.68200,
$
l$tab

```

```

                                /table of mu/(Rearth+altito)^2-veli^2/(Rearth+altito)
                                /multiplied above by mass
table = 6hgenv4t, 2, 6hveli , 6haltito , 16, 13, 1, 1, 1, 1, 1, 1, 1, 1,
50000,
5000, 5.75727, 5200, 5.43991, 5400, 5.11011, 5600, 4.76787,
5800, 4.41318, 6000, 4.04604, 6200, 3.66646, 6400, 3.27444,
6600, 2.86997, 6800, 2.45305, 7000, 2.02369, 7200, 1.58188,

```

7400, 1.12763, 7600, 0.66093, 7800, 0.18179, 8000, -0.30980,  
 55000,  
 5000, 5.74530, 5200, 5.42819, 5400, 5.09865, 5600, 4.75667,  
 5800, 4.40226, 6000, 4.03541, 6200, 3.65612, 6400, 3.26440,  
 6600, 2.86024, 6800, 2.44365, 7000, 2.01462, 7200, 1.57316,  
 7400, 1.11926, 7600, 0.65293, 7800, 0.17415, 8000, -0.31705,  
 60000,  
 5000, 5.73337, 5200, 5.41650, 5400, 5.08722, 5600, 4.74550,  
 5800, 4.39136, 6000, 4.02480, 6200, 3.64581, 6400, 3.25439,  
 6600, 2.85055, 6800, 2.43428, 7000, 2.00558, 7200, 1.56446,  
 7400, 1.11092, 7600, 0.64494, 7800, 0.16655, 8000, -0.32428,  
 65000,  
 5000, 5.72146, 5200, 5.40484, 5400, 5.07581, 5600, 4.73436,  
 5800, 4.38050, 6000, 4.01422, 6200, 3.63552, 6400, 3.24441,  
 6600, 2.84088, 6800, 2.42493, 7000, 1.99657, 7200, 1.55579,  
 7400, 1.10260, 7600, 0.63699, 7800, 0.15896, 8000, -0.33148,  
 70000,  
 5000, 5.70958, 5200, 5.39321, 5400, 5.06444, 5600, 4.72325,  
 5800, 4.36966, 6000, 4.00367, 6200, 3.62526, 6400, 3.23445,  
 6600, 2.83124, 6800, 2.41561, 7000, 1.98758, 7200, 1.54715,  
 7400, 1.09430, 7600, 0.62905, 7800, 0.15140, 8000, -0.33867,  
 75000,  
 5000, 5.69774, 5200, 5.38161, 5400, 5.05309, 5600, 4.71217,  
 5800, 4.35886, 6000, 3.99314, 6200, 3.61503, 6400, 3.22453,  
 6600, 2.82162, 6800, 2.40632, 7000, 1.97862, 7200, 1.53853,  
 7400, 1.08603, 7600, 0.62114, 7800, 0.14386, 8000, -0.34583,  
 80000,  
 5000, 5.68592, 5200, 5.37004, 5400, 5.04177, 5600, 4.70112,  
 5800, 4.34808, 6000, 3.98265, 6200, 3.60483, 6400, 3.21462,  
 6600, 2.81203, 6800, 2.39705, 7000, 1.96968, 7200, 1.52993,  
 7400, 1.07779, 7600, 0.61326, 7800, 0.13634, 8000, -0.35296,  
 85000,  
 5000, 5.67414, 5200, 5.35850, 5400, 5.03049, 5600, 4.69009,  
 5800, 4.33733, 6000, 3.97218, 6200, 3.59465, 6400, 3.20475,  
 6600, 2.80247, 6800, 2.38781, 7000, 1.96077, 7200, 1.52136,  
 7400, 1.06957, 7600, 0.60540, 7800, 0.12885, 8000, -0.36008,  
 90000,  
 5000, 5.66238, 5200, 5.34699, 5400, 5.01923, 5600, 4.67910,  
 5800, 4.32660, 6000, 3.96174, 6200, 3.58450, 6400, 3.19490,  
 6600, 2.79293, 6800, 2.37859, 7000, 1.95189, 7200, 1.51281,  
 7400, 1.06137, 7600, 0.59756, 7800, 0.12138, 8000, -0.36717,  
 95000,  
 5000, 5.65065, 5200, 5.33550, 5400, 5.00800, 5600, 4.66813,  
 5800, 4.31591, 6000, 3.95132, 6200, 3.57438, 6400, 3.18508,  
 6600, 2.78342, 6800, 2.36940, 7000, 1.94303, 7200, 1.50429,

```

7400, 1.05320, 7600, 0.58974, 7800, 0.11393, 8000, -0.37424,
100000,
5000, 5.63895, 5200, 5.32405, 5400, 4.99679, 5600, 4.65719,
5800, 4.30524, 6000, 3.94094, 6200, 3.56429, 6400, 3.17529,
6600, 2.77394, 6800, 2.36024, 7000, 1.93419, 7200, 1.49579,
7400, 1.04505, 7600, 0.58195, 7800, 0.10651, 8000, -0.38129,
105000,
5000, 5.62729, 5200, 5.31262, 5400, 4.98562, 5600, 4.64628,
5800, 4.29460, 6000, 3.93058, 6200, 3.55422, 6400, 3.16552,
6600, 2.76448, 6800, 2.35110, 7000, 1.92538, 7200, 1.48732,
7400, 1.03692, 7600, 0.57418, 7800, 0.09910, 8000, -0.38831,
110000,
5000, 5.61565, 5200, 5.30123, 5400, 4.97448, 5600, 4.63540,
5800, 4.28399, 6000, 3.92025, 6200, 3.54418, 6400, 3.15577,
6600, 2.75504, 6800, 2.34198, 7000, 1.91659, 7200, 1.47887,
7400, 1.02882, 7600, 0.56644, 7800, 0.09173, 8000, -0.39532,
ixtrp = 0,0,0,0,
$
l$tab

```

table /table of bank angle as a function of genv2/genv1. The

```

/is actually acos(rgenv)
table = 6hbankt , 1, 6hrgenv , 201, 1, 1, 1,
-1.00, 180.000000, -0.99, 171.890386, -0.98, 168.521659, -0.97, 165.930132,
-0.96, 163.739795, -0.95, 161.805128, -0.94, 160.051556, -0.93, 158.434815,
-0.92, 156.926082, -0.91, 155.505352, -0.90, 154.158067, -0.89, 152.873247,
-0.88, 151.642363, -0.87, 150.458639, -0.86, 149.316583, -0.85, 148.211669,
-0.84, 147.140120, -0.83, 146.098738, -0.82, 145.084794, -0.81, 144.095931,
-0.80, 143.130102, -0.79, 142.185511, -0.78, 141.260575, -0.77, 140.353889,
-0.76, 139.464198, -0.75, 138.590378, -0.74, 137.731416, -0.73, 136.886394,
-0.72, 136.054480, -0.71, 135.234915, -0.70, 134.427004, -0.69, 133.630109,
-0.68, 132.843643, -0.67, 132.067065, -0.66, 131.299873, -0.65, 130.541602,
-0.64, 129.791819, -0.63, 129.050123, -0.62, 128.316134, -0.61, 127.589503,
-0.60, 126.869898, -0.59, 126.157008, -0.58, 125.450543, -0.57, 124.750226,
-0.56, 124.055798, -0.55, 123.367013, -0.54, 122.683639, -0.53, 122.005455,
-0.52, 121.332251, -0.51, 120.663830, -0.50, 120.000000, -0.49, 119.340582,
-0.48, 118.685402, -0.47, 118.034297, -0.46, 117.387108, -0.45, 116.743684,
-0.44, 116.103881, -0.43, 115.467560, -0.42, 114.834587, -0.41, 114.204835,
-0.40, 113.578178, -0.39, 112.954499, -0.38, 112.333683, -0.37, 111.715617,
-0.36, 111.100196, -0.35, 110.487315, -0.34, 109.876874, -0.33, 109.268775,
-0.32, 108.662925, -0.31, 108.059230, -0.30, 107.457603, -0.29, 106.857956,
-0.28, 106.260205, -0.27, 105.664267, -0.26, 105.070062, -0.25, 104.477512,
-0.24, 103.886540, -0.23, 103.297072, -0.22, 102.709033, -0.21, 102.122352,
-0.20, 101.536959, -0.19, 100.952784, -0.18, 100.369760, -0.17, 99.787819,

```

```

-0.16, 99.206896, -0.15, 98.626927, -0.14, 98.047846, -0.13, 97.469592,
-0.12, 96.892103, -0.11, 96.315316, -0.10, 95.739170, -0.09, 95.163607,
-0.08, 94.588566, -0.07, 94.013987, -0.06, 93.439813, -0.05, 92.865984,
-0.04, 92.292443, -0.03, 91.719131, -0.02, 91.145992, -0.01, 90.572967,
0.00, 90.000000, 0.01, 89.427033, 0.02, 88.854008, 0.03, 88.280869,
0.04, 87.707557, 0.05, 87.134016, 0.06, 86.560187, 0.07, 85.986013,
0.08, 85.411434, 0.09, 84.836393, 0.10, 84.260830, 0.11, 83.684684,
0.12, 83.107897, 0.13, 82.530408, 0.14, 81.952154, 0.15, 81.373073,
0.16, 80.793104, 0.17, 80.212181, 0.18, 79.630240, 0.19, 79.047216,
0.20, 78.463041, 0.21, 77.877648, 0.22, 77.290967, 0.23, 76.702928,
0.24, 76.113460, 0.25, 75.522488, 0.26, 74.929938, 0.27, 74.335733,
0.28, 73.739795, 0.29, 73.142044, 0.30, 72.542397, 0.31, 71.940770,
0.32, 71.337075, 0.33, 70.731225, 0.34, 70.123126, 0.35, 69.512685,
0.36, 68.899804, 0.37, 68.284383, 0.38, 67.666317, 0.39, 67.045501,
0.40, 66.421822, 0.41, 65.795165, 0.42, 65.165413, 0.43, 64.532440,
0.44, 63.896119, 0.45, 63.256316, 0.46, 62.612892, 0.47, 61.965703,
0.48, 61.314598, 0.49, 60.659418, 0.50, 60.000000, 0.51, 59.336170,
0.52, 58.667749, 0.53, 57.994545, 0.54, 57.316361, 0.55, 56.632987,
0.56, 55.944202, 0.57, 55.249774, 0.58, 54.549457, 0.59, 53.842992,
0.60, 53.130102, 0.61, 52.410497, 0.62, 51.683866, 0.63, 50.949877,
0.64, 50.208181, 0.65, 49.458398, 0.66, 48.700127, 0.67, 47.932935,
0.68, 47.156357, 0.69, 46.369891, 0.70, 45.572996, 0.71, 44.765085,
0.72, 43.945520, 0.73, 43.113606, 0.74, 42.268584, 0.75, 41.409622,
0.76, 40.535802, 0.77, 39.646111, 0.78, 38.739425, 0.79, 37.814489,
0.80, 36.869898, 0.81, 35.904069, 0.82, 34.915206, 0.83, 33.901262,
0.84, 32.859880, 0.85, 31.788331, 0.86, 30.683417, 0.87, 29.541361,
0.88, 28.357637, 0.89, 27.126753, 0.90, 25.841933, 0.91, 24.494648,
0.92, 23.073918, 0.93, 21.565185, 0.94, 19.948444, 0.95, 18.194872,
0.96, 16.260205, 0.97, 14.069868, 0.98, 11.478341, 0.99, 8.109614,
1.00, 0.000000,
ixtrp = 0,0,0,0,
$
l$tab
table = 5htvc1t, 0, 14679.0,
$
l$tab

```

/table of thrust as a function of alpha. Table is  
/1/cos(alpha)multiplied above by drag.

```

table = 6hetat , 1, 6halph , 44, 1,1,1,
0,1.00000, 1,1.00015, 2,1.00061, 3,1.00137,
4,1.00244, 5,1.00382, 6,1.00551, 7,1.00751,
8,1.00983, 9,1.01247, 10,1.01543, 11,1.01872,
12,1.02234, 13,1.02630, 14,1.03061, 15,1.03528,
16,1.04030, 17,1.04569, 18,1.05146, 19,1.05762,

```



```

20,1.06418, 21,1.07114, 22,1.07853, 23,1.08636,
24,1.09464, 25,1.10338, 26,1.11260, 27,1.12233,
28,1.13257, 29,1.14335, 30,1.15470, 31,1.16663,
32,1.17918, 33,1.19236, 34,1.20622, 35,1.22077,
36,1.23607, 37,1.25214, 38,1.26902, 39,1.28676,
40,1.30541, 41,1.32501, 42,1.34563, 43,1.36733,
ixtrp = 0,0,0,0,
endphs = 1,
$
l$gendat
event = 60, /Ascend to top of atmosphere
critr = 6htdurp, /length of heat control
npc(8) = 2, /aero coeff in tables
npc(9) = 1, /rocket engine
iwdf = 2, /calculate using isp and thrust
ispv = 300.0, /isp
iengmf = 0, /turn off rocket engine
npc(15) = 1, /aeroheating
iguid = 0, 1, 0, /aero angles guidance
iguid(6) = 1, 0, 1,
npc(22) = 0, /no more throttling parameter
eta = 1,
bnkarg = 6htdurp,
alparg = 6htdurp,
$
l$tblmlt
$
l$tab
table = 5htvc1t, 0, 14679.0,
endphs = 1,
$
l$gendat
event = 60.1, /thrust if needed
critr = 6htdurp, /start thrusting after 50 seconds
value = 50,
npc(8) = 2, /aero coeff in tables
npc(9) = 1, /rocket engine
iwdf = 2, /calculate using isp and thrust
ispv = 300.0, /isp
iengmf = 1, /turn on rocket engine
npc(15) = 1, /aeroheating
iguid = 0, 1, 0, /aero angles guidance
iguid(6) = 1, 0, 1,
$
l$tblmlt

```

```

$
l$tab
table = 5htvc1t, 0, 14679.0,
endphs = 1,
$
l$gendat
event = 60.2, /stop thrust when no longer needed
critr = 6halta,
value = 120.0,
npc(8) = 2, /aero coeff in tables
npc(9) = 1, /rocket engine
iwdf = 2, /calculate using isp and thrust
ispv = 300.0, /isp
iengmf = 0, /turn off rocket engine
npc(15) = 1, /aeroheating
iguid = 0, 1, 0, /aero angles guidance
iguid(6) = 1, 0, 1,
$
l$tblmlt
$
l$tab
table = 5htvc1t, 0, 14679.0,
endphs = 1,
$
l$gendat
event = 80, /EXIT ATMOSPHERE
critr = 6haltito,
value = 111000.0,
npc(5) = 0, /no atmosphere
npc(8) = 0, /no aero coeff
iengmf = 0, /turn off rocket engine
iguid = 0, 1, 0, /aero angles guidance
iguid(6) = 1, 1, 1,
banki = 0,
alphi = 0,
betai = 0,
betpc = 0, 0, 0, 0,
alppc = 0, 0, 0, 0,
bnkpc = 0, 0, 0, 0,
endphs = 1,
$
l$gendat
event = 80.1, /START REORBIT IMPULSE
critr = 6hgammai, /Start the impulse if gamma=0
value = 0,

```

```

npc(9) = 1,           /rocket engine
npc(5) = 0,           /no atmosphere
npc(8) = 0,           /no aero coeff
iwdf = 2,             /calculate using isp and thrust
ispv = 300,
iengmf = 1,           /turn on rocket engine
$
l$tblmlt
$
l$tab
table = 5htvc1t, 0, 1500000.0, /1000 times normal max thrust
endphs = 1,
$
l$gendat
event = 80.2,         /STOP REORBIT IMPULSE
critr = 6halta,       /stop the impulse when apogee=185km
value = 185.1,
npc(2) = 3,           /Laplace conic integration method
dt = 100,
prnc = 200,           /print interval 200 sec
prnca = 200,
pinc = 200,
npc(5) = 0,           /no atmosphere
npc(8) = 0,           /no aero coeff
iengmf = 0,           /turn off rocket engine
iwdf = 2,             /calculate using isp and thrust
$
l$tblmlt
$
l$tab
table = 5htvc1t, 0, 1500000.0,
endphs = 1,
$
l$gendat
event = 90,           /CIRCULARIZATION IMPULSE
critr = 6haltito,
value = 185000.0,
npc(9) = 3,
ispv = 300,
isdvin = 0.0,
endphs = 1,
$
l$gendat
event = 100,          /END RUN
critr = 6htdurp,

```

```
value = 5.0,  
endphs = 1,  
endprb = 1,  
endjob = 1,  
$
```

## APPENDIX C. MAPLE PROGRAM OUTPUT

The following file is an example of the output used from the MAPLE ® symbolic manipulation program for generating the equations for the indirect analysis. In this file some commands were used to actually calculate the equations while others were purely to produce output to cut and paste into the thesis.

> with(linalg):

Warning: new definition for norm  
Warning: new definition for trace

> x:=vector([r,v,gamma,phi,psi,m]);

$$x = [r \quad v \quad \gamma \quad \phi \quad \psi \quad m]$$

> lambda:=vector([lambda[r],lambda[v],lambda[gamma],lambda[phi],lambda[psi],lambda[m]]);

$$\lambda = \begin{bmatrix} \lambda_r & \lambda_v & \lambda_\gamma & \lambda_\phi & \lambda_\psi & \lambda_m \end{bmatrix}$$

> x:=vector([r,v,gamma,phi,psi,m,lambda[r],lambda[v],lambda[gamma],lambda[phi],lambda[psi],lambda[m]]);

$$x := \begin{bmatrix} r & v & \gamma & \phi & \psi & m & \lambda_r & \lambda_v & \lambda_\gamma & \lambda_\phi & \lambda_\psi & \lambda_m \end{bmatrix}$$

> u:=vector([T,alpha,delta]);

$$u = [T \quad \alpha \quad \delta]$$

> dx/dt=f(x,u,t);

$$\frac{dx}{dt} = f(x, u, t)$$

> f:=vector(14);

$$f := \text{array}(1 \dots 14, [ \ ])$$

> d1:=D(alpha);

$$d1 := D(\alpha)$$

> l:=L(alpha);

$$l := L(\alpha)$$

> deltaVb:=sqrt(2\*mu\*(1/Ra-1/Rc)/(1-(Ra/Rc)^2\*cos(gamma[f]^2))-V[f];

$$\text{deltaVb} := \sqrt{2} \sqrt{\frac{\mu \left( \frac{1}{Ra} - \frac{1}{Rc} \right)}{Ra^2 \cos(\gamma_f)^2 - 1 - \frac{Rc^2}{Ra^2 \cos(\gamma_f)^2}} - V_f}$$

> deltaVc:=sqrt(mu/Rc)-sqrt(2\*mu\*(1/Ra-1/Rc)/((Rc/Ra)^2/cos(gamma[f]^2-1));

$$\text{deltaVc} := \sqrt{\frac{\mu}{Rc}} - \sqrt{2} \sqrt{\frac{\mu \left( \frac{1}{Ra} - \frac{1}{Rc} \right)}{Ra^2 \cos(\gamma_f)^2 - 1 - \frac{Rc^2}{Ra^2 \cos(\gamma_f)^2}}}$$

> f[1]:=v\*sin(gamma);

$$f_1 := v \sin(\gamma)$$

> dr/dt=v\*sin(gamma);

$$\frac{dr}{dt} = v \sin(\gamma)$$

$$> As := (T \cos(\alpha) - D) / m;$$

$$As := \frac{T \cos(\alpha) - D(\alpha)}{m}$$

$$> f[2] := As - g \sin(\gamma);$$

$$f_2 := \frac{T \cos(\alpha) - D(\alpha)}{m} - g \sin(\gamma)$$

$$> dv/dt = As - g \sin(\gamma);$$

$$\frac{dv}{dt} = \frac{T \cos(\alpha) - D(\alpha)}{m} - g \sin(\gamma)$$

$$> Ar := (L + T \sin(\alpha)) \cos(\delta) / m;$$

$$Ar := \frac{(L(\alpha) + T \sin(\alpha)) \cos(\delta)}{m}$$

$$> f[3] := (Ar - g \cos(\gamma) + v^2 \cos(\gamma) / r) / v;$$

$$f_3 := \frac{\frac{(L(\alpha) + T \sin(\alpha)) \cos(\delta)}{m} - g \cos(\gamma) + \frac{v^2 \cos(\gamma)}{r}}{v}$$

$$> v \cdot d\gamma/dt = (Ar - g \cos(\gamma) + v^2 \cos(\gamma) / r);$$

$$\frac{v d\gamma}{dt} = \frac{(L(\alpha) + T \sin(\alpha)) \cos(\delta)}{m} - g \cos(\gamma) + \frac{v^2 \cos(\gamma)}{r}$$

$$> f[4] := v \cos(\gamma) \sin(\psi) / r;$$

$$f_4 := \frac{v \cos(\gamma) \sin(\psi)}{r}$$

$$> d\phi/dt = v \cos(\gamma) \sin(\psi) / r;$$

$$\frac{d\phi}{dt} = \frac{v \cos(\gamma) \sin(\psi)}{r}$$

$$> Aw := (L + T \sin(\alpha)) \sin(\delta) / m;$$

$$Aw := \frac{(L(\alpha) + T \sin(\alpha)) \sin(\delta)}{m}$$

$$> f[5] := (Aw / \cos(\gamma) - v^2 / r \cos(\gamma) \cos(\psi) \tan(\phi)) / v;$$

$$f_5 := \frac{\frac{(L(\alpha) + T \sin(\alpha)) \sin(\delta)}{m \cos(\gamma)} - \frac{v^2 \cos(\gamma) \cos(\psi) \tan(\phi)}{r}}{v}$$

$$> v \cdot d\psi/dt = (Aw / \cos(\gamma) - v^2 / r \cos(\gamma) \cos(\psi) \tan(\phi));$$

$$\frac{v d\psi}{dt} = \frac{(L(\alpha) + T \sin(\alpha)) \sin(\delta)}{m \cos(\gamma)} - \frac{v^2 \cos(\gamma) \cos(\psi) \tan(\phi)}{r}$$

$$> f[6] := T / Isp \cdot g_0;$$

$$f_6 := -\frac{T}{Isp \cdot g_0}$$

$$> dm/dt = -T / Isp \cdot g_0;$$

$$\frac{dm}{dt} = -\frac{T}{I_{sp} g_0}$$

> g:=mu/r^2;

$$g := \frac{\mu}{r^2}$$

> q1:=(2\*T/T[max]-1)^z+(2\*alpha/alpha[max]-1)^z-1;

$$q1 := \left( 2 \frac{T}{T_{max}} - 1 \right)^z + \left( 2 \frac{\alpha}{\alpha_{max}} - 1 \right)^z - 1$$

> G:=C\*rho0\*exp(-beta\*N\*r)\*v^M-qdot[max];

$$G := C \rho_0 e^{(-\beta N r)} v^M - qdot_{max}$$

> p:=T\*cos(alpha)-D(alpha)-m\*sin(gamma)\*(mu/r^2+xi\*v^2);

$$p = T \cos(\alpha) - D(\alpha) - m \sin(\gamma) \left( \frac{\mu}{r^2} + \xi v^2 \right)$$

> p:=T\*cos(alpha)-D(alpha)-m\*sin(gamma)\*(mu/r^2+xi\*v^2);

$$p := T \cos(\alpha) - D(\alpha) - m \sin(\gamma) \left( \frac{\mu}{r^2} + \xi v^2 \right)$$

> h:=0;

$$h := 0$$

> for s from 1 to 6 do;h:=h+x[s+6]\*f[s];od;

> L=h-kappa\*q1-eta\*p;

$$\begin{aligned} L = & \lambda_r v \sin(\gamma) + \lambda_v \left( \frac{T \cos(\alpha) - D(\alpha)}{m} - \frac{\mu \sin(\gamma)}{r^2} \right) \\ & + \frac{\lambda_\gamma \left( \frac{(L(\alpha) + T \sin(\alpha)) \cos(\delta)}{m} - \frac{\mu \cos(\gamma)}{r^2} + \frac{v^2 \cos(\gamma)}{r} \right)}{v} + \frac{\lambda_\phi v \cos(\gamma) \sin(\psi)}{r} \\ & + \frac{\lambda_\psi \left( \frac{(L(\alpha) + T \sin(\alpha)) \sin(\delta)}{m \cos(\gamma)} - \frac{v^2 \cos(\gamma) \cos(\psi) \tan(\phi)}{r} \right)}{v} - \frac{\lambda_m T}{I_{sp} g_0} \\ & - \kappa \left( \left( 2 \frac{T}{T_{max}} - 1 \right)^z + \left( 2 \frac{\alpha}{\alpha_{max}} - 1 \right)^z - 1 \right) \\ & - \eta \left( T \cos(\alpha) - D(\alpha) - m \sin(\gamma) \left( \frac{\mu}{r^2} + \xi v^2 \right) \right) \end{aligned}$$

> c:=h-kappa\*q1-eta\*p;



$$\begin{aligned}
c := & \lambda_r v \sin(\gamma) + \lambda_v \left( \frac{T \cos(\alpha) - D(\alpha)}{m} - \frac{\mu \sin(\gamma)}{r^2} \right) \\
& + \frac{\lambda_\gamma \left( \frac{(L(\alpha) + T \sin(\alpha)) \cos(\delta)}{m} - \frac{\mu \cos(\gamma)}{r^2} + \frac{v^2 \cos(\gamma)}{r} \right)}{v} + \frac{\lambda_\phi v \cos(\gamma) \sin(\psi)}{r} \\
& + \frac{\lambda_\psi \left( \frac{(L(\alpha) + T \sin(\alpha)) \sin(\delta)}{m \cos(\gamma)} - \frac{v^2 \cos(\gamma) \cos(\psi) \tan(\phi)}{r} \right)}{v} - \frac{\lambda_m T}{Isp g0} \\
& - \kappa \left( \left( 2 \frac{T}{T_{max}} - 1 \right)^2 + \left( 2 \frac{\alpha}{\alpha_{max}} - 1 \right)^2 - 1 \right) \\
& - \eta \left( T \cos(\alpha) - D(\alpha) - m \sin(\gamma) \left( \frac{\mu}{r^2} + \xi v^2 \right) \right)
\end{aligned}$$

> for s from 1 to 6 do;f[s+6]:=0;od;

> for s from 1 to 6 do;f[s+6]:=diff(c,x[s]);od;

> Diff(lambda[r],t)=subs({diff(lambda[r],r)=0},f[7]);

$$\begin{aligned}
\frac{\partial}{\partial t} \lambda_r = & -2 \frac{\lambda_v \mu \sin(\gamma)}{r^3} - \frac{\lambda_\gamma \left( 2 \frac{\mu \cos(\gamma)}{r^3} - \frac{v^2 \cos(\gamma)}{r^2} \right)}{v} + \frac{\lambda_\phi v \cos(\gamma) \sin(\psi)}{r^2} \\
& - \frac{\lambda_\psi v \cos(\gamma) \cos(\psi) \tan(\phi)}{r^2} + 2 \frac{\eta m \sin(\gamma) \mu}{r^3}
\end{aligned}$$

lambda1dot

> Diff(lambda[v],t)=subs({diff(lambda[v],v)=0},f[8]);

$$\begin{aligned}
\frac{\partial}{\partial t} \lambda_v = & -\lambda_r \sin(\gamma) - 2 \frac{\lambda_\gamma \cos(\gamma)}{r} + \frac{\lambda_\gamma \left( \frac{(L(\alpha) + T \sin(\alpha)) \cos(\delta)}{m} - \frac{\mu \cos(\gamma)}{r^2} + \frac{v^2 \cos(\gamma)}{r} \right)}{v^2} \\
& - \frac{\lambda_\phi \cos(\gamma) \sin(\psi)}{r} + 2 \frac{\lambda_\psi \cos(\gamma) \cos(\psi) \tan(\phi)}{r} \\
& + \frac{\lambda_\psi \left( \frac{(L(\alpha) + T \sin(\alpha)) \sin(\delta)}{m \cos(\gamma)} - \frac{v^2 \cos(\gamma) \cos(\psi) \tan(\phi)}{r} \right)}{v^2} - 2 \eta m \sin(\gamma) \xi v
\end{aligned}$$

lambda2dot

> Diff(lambda[gamma],t)=subs({diff(lambda[gamma],gamma)=0},f[9]);

$$\begin{aligned} \frac{\partial}{\partial t} \lambda_{\gamma} = & -\lambda_{\gamma} \frac{v \cos(\gamma)}{r} + \frac{\lambda_{\gamma} \mu \cos(\gamma)}{r^2} - \frac{\lambda_{\gamma} \left( \frac{\mu \sin(\gamma)}{r^2} - \frac{v^2 \sin(\gamma)}{r} \right)}{v} + \frac{\lambda_{\phi} v \sin(\gamma) \sin(\psi)}{r} \\ & - \frac{\lambda_{\psi} \left( \frac{(L(\alpha) + T \sin(\alpha)) \sin(\delta) \sin(\gamma)}{m \cos(\gamma)^2} + \frac{v^2 \sin(\gamma) \cos(\psi) \tan(\phi)}{r} \right)}{v} \\ & - \eta m \cos(\gamma) \left( \frac{\mu}{r^2} + \xi v^2 \right) \end{aligned}$$

lambda3dot

> Diff(lambda[phi],t)=subs({diff(lambda[phi],phi)=0},f[10]);

$$\frac{\partial}{\partial t} \lambda_{\phi} = \frac{\lambda_{\psi} v \cos(\gamma) \cos(\psi) (1 + \tan(\phi)^2)}{r}$$

lambda4dot

> Diff(lambda[psi],t)=subs({diff(lambda[psi],psi)=0},f[11]);

$$\frac{\partial}{\partial t} \lambda_{\psi} = -\frac{\lambda_{\phi} v \cos(\gamma) \cos(\psi)}{r} - \frac{\lambda_{\psi} v \cos(\gamma) \sin(\psi) \tan(\phi)}{r}$$

lambda5dot

> Diff(lambda[m],t)=subs({diff(lambda[m],m)=0},f[12]);

$$\begin{aligned} \frac{\partial}{\partial t} \lambda_m = & \frac{\lambda_v (T \cos(\alpha) - D(\alpha))}{m^2} + \frac{\lambda_{\gamma} (L(\alpha) + T \sin(\alpha)) \cos(\delta)}{m^2 v} \\ & + \frac{\lambda_{\psi} (L(\alpha) + T \sin(\alpha)) \sin(\delta)}{m^2 \cos(\gamma) v} - \eta \sin(\gamma) \left( \frac{\mu}{r^2} + \xi v^2 \right) \end{aligned}$$

lambda6dot

> Diff(L,T)=diff(c,T);

$$\begin{aligned} \frac{\partial}{\partial T} L = & \frac{\lambda_v \cos(\alpha)}{m} + \frac{\lambda_{\gamma} \sin(\alpha) \cos(\delta)}{m v} + \frac{\lambda_{\psi} \sin(\alpha) \sin(\delta)}{m \cos(\gamma) v} - \frac{\lambda_m}{Isp g0} - 2 \frac{\kappa \left( 2 \frac{T}{T_{max}} - 1 \right)^z}{T_{max} \left( 2 \frac{T}{T_{max}} - 1 \right)} \\ & - \eta \cos(\alpha) \end{aligned}$$

> Diff(Diff(L,T),T)=subs(diff(T[max],T)=0,diff(diff(c,T),T));

$$\frac{\partial^2}{\partial T^2} L = -4 \frac{\kappa \left( 2 \frac{T}{T_{max}} - 1 \right)^z z^2}{T_{max}^2 \left( 2 \frac{T}{T_{max}} - 1 \right)^2} + 4 \frac{\kappa \left( 2 \frac{T}{T_{max}} - 1 \right)^z z}{T_{max}^2 \left( 2 \frac{T}{T_{max}} - 1 \right)^2}$$

> Diff(L,delta)=diff(c,delta);

$$\frac{\partial}{\partial \delta} L = - \frac{\lambda_{\gamma} (L(\alpha) + T \sin(\alpha)) \sin(\delta)}{m v} + \frac{\lambda_{\psi} (L(\alpha) + T \sin(\alpha)) \cos(\delta)}{m \cos(\gamma) v}$$

> Diff(L,alpha)=diff(c,alpha);

$$\begin{aligned} \frac{\partial}{\partial \alpha} L = & \frac{\lambda_{\nu} \left( -T \sin(\alpha) - \left( \frac{\partial}{\partial \alpha} D(\alpha) \right) \right)}{m} + \frac{\lambda_{\gamma} \left( \left( \frac{\partial}{\partial \alpha} L(\alpha) \right) + T \cos(\alpha) \right) \cos(\delta)}{m v} \\ & + \frac{\lambda_{\psi} \left( \left( \frac{\partial}{\partial \alpha} L(\alpha) \right) + T \cos(\alpha) \right) \sin(\delta)}{m \cos(\gamma) v} - 2 \frac{\kappa \left( 2 \frac{\alpha}{\alpha_{max}} - 1 \right)^z z}{\alpha_{max} \left( 2 \frac{\alpha}{\alpha_{max}} - 1 \right)} \\ & - \eta \left( -T \sin(\alpha) - \left( \frac{\partial}{\partial \alpha} D(\alpha) \right) \right) \end{aligned}$$

> Diff(Diff(L,alpha),alpha)=diff(diff(c,alpha),alpha);

$$\begin{aligned} \frac{\partial^2}{\partial \alpha^2} L = & \frac{\lambda_{\nu} \left( -T \cos(\alpha) - \left( \frac{\partial^2}{\partial \alpha^2} D(\alpha) \right) \right)}{m} + \frac{\lambda_{\gamma} \left( \left( \frac{\partial^2}{\partial \alpha^2} L(\alpha) \right) - T \sin(\alpha) \right) \cos(\delta)}{m v} \\ & + \frac{\lambda_{\psi} \left( \left( \frac{\partial^2}{\partial \alpha^2} L(\alpha) \right) - T \sin(\alpha) \right) \sin(\delta)}{m \cos(\gamma) v} - 4 \frac{\kappa \left( 2 \frac{\alpha}{\alpha_{max}} - 1 \right)^z z^2}{\alpha_{max}^2 \left( 2 \frac{\alpha}{\alpha_{max}} - 1 \right)^2} \\ & + 2 \frac{\kappa \left( 2 \frac{\alpha}{\alpha_{max}} - 1 \right)^z z \left( \frac{\partial}{\partial \alpha} \alpha_{max} \right)}{\alpha_{max}^2 \left( 2 \frac{\alpha}{\alpha_{max}} - 1 \right)} + 4 \frac{\kappa \left( 2 \frac{\alpha}{\alpha_{max}} - 1 \right)^z z}{\alpha_{max}^2 \left( 2 \frac{\alpha}{\alpha_{max}} - 1 \right)^2} \end{aligned}$$

$$- \eta \left( -T \cos(\alpha) - \left( \frac{\partial^2}{\partial \alpha^2} D(\alpha) \right) \right)$$

> D(alpha):=Q\*(Cd0+2\*sin(alpha)^3);

$$D(\alpha) := Q (Cd0 + 2 \sin(\alpha)^3)$$

> L(alpha):=Q\*(2\*sin(alpha)^2\*cos(alpha));

$$L(\alpha) := 2 Q \sin(\alpha)^2 \cos(\alpha)$$

*These are the newtonian values for the L and D functions for a flat plate.*

> xf:=vector([r[f],v[f],gamma[f],phi[f],psi[f],m[f]]);

$$xf := \begin{bmatrix} r_f & v_f & \gamma_f & \phi_f & \psi_f & m_f \end{bmatrix}$$

> F:=vector([cos(psi[f])\*cos(phi[f])-cos(i[f]),r[top]-r[f],v[top]-v[f],gamma[top]-gamma[f]]);

$$F := \begin{bmatrix} \cos(\psi_f) \cos(\phi_f) - \cos(i_f) & r_{top} - r_f & v_{top} - v_f & \gamma_{top} - \gamma_f \end{bmatrix}$$

> J:=m1;

$$J := -m l$$

> nu:=vector(4);

$$v := \text{array}(1 \dots 4, [ \ ])$$

> for n from 1 to 6 do:

> lambdatf[n]:=diff(J,xf[n]);

> for s from 1 to 4 do:

> lambdatf[n]:=lambdatf[n]+nu[s]\*diff(F[s],xf[n]);

> od:

> od:

> for n from 1 to 6 do: lambdatf[n];od;

$$-v_2$$

$$-v_3$$

$$-v_4$$

$$-v_1 \cos(\psi_f) \sin(\phi_f)$$

$$-v_1 \sin(\psi_f) \cos(\phi_f)$$

$$0$$

*Now I will try to look at the jump conditions from constrained to unconstrained. The applicable condition to transition from unconstrained to constrained is continuity in lambda.*

> for n from 1 to 6 do

>  $\lambda_{daa}[n] = \lambda_{dab}[n] - \eta C \rho_0 \beta N e^{(-\beta N r)} \nu M$ ;od;

$$\lambda_{daa}_1 = \lambda_{dab}_1 + \eta C \rho_0 \beta N e^{(-\beta N r)} \nu M$$

$$\lambda_{daa}_2 = \lambda_{dab}_2 - \frac{\eta C \rho_0 e^{(-\beta N r)} \nu M}{v}$$

$$\lambda_{daa}_3 = \lambda_{dab}_3$$

$$\lambda_{daa}_4 = \lambda_{dab}_4$$

$$\lambda_{daa}_5 = \lambda_{dab}_5$$

$$\lambda_{daa}_6 = \lambda_{dab}_6$$

>



## LIST OF REFERENCES

- 1 Nicholson, J. C., *Numerical Optimization of Synergetic Maneuvers*, Master's Thesis, Naval Postgraduate School, 1994.
- 2 Spriesterbach, T. P., *Performance Analysis of Non-Coplanar Synergetic Maneuvers*, Master's Thesis, Naval Postgraduate School, 1991.
- 3 Lee, J. Y. and Hull, D. G., "Maximum Orbit Plane Change with Heat-Transfer-Rate Considerations", *Journal of Guidance, Control, and Dynamics*, Vol. 13, No. 3, 1990, pp. 492-497.
- 4 Hull, D. G., and Speyer, J. L., "Optimal Reentry and Plane Change Trajectories", *The Journal of Astronautical Sciences*, Vol. 30, No. 2, 1982, pp. 117-130.
- 5 Miele, A., and Lee, W. Y., "Optimal Trajectories for Hypervelocity Flight", American Control Conference Proceedings, June 21-23, 1989.
- 6 Mishne, D., and Hougui, S., "An Approximate Guidance Law for Atmospheric Plane Change Maneuver of an Aerocruise Space Vehicle", AIAA Atmospheric Flight Conference Proceedings, Aug. 20-22, 1990.
- 7 Mease, K. D., "Optimization of Aeroassisted Orbital Transfer: Current Status", *The Journal of Astronautical Sciences*, Vol. 36, Nos. 1/2, Jan-June 1988, pp. 7-33.
- 8 Gord, R., Personal Telephone Conversation, Air Force Flight Dynamics Laboratory, Wright Patterson AFB, Oct. 1995.
- 9 Bryson, A. E., and Ho, Y., *Applied Optimal Control*, Halsted Press, New York, 1975.
- 10 Pontryagin, L. S., Boltyanskii, V. G., Gamkrelidze, R. V., Mishchenko, E. F., *The Mathematical Theory of Optimal Processes*, Interscience Publishers, New York, 1962.
- 11 Knowles, G., *An Introduction to Applied Optimal Control*, Academic Press, New York, 1981.
- 12 Brauer, G. L., Cornick, D. E., Olson, D. W., Peterson, F. M., and Stevenson, R., *Program to Optimize Simulated Trajectories (POST)*, Vol. I, Martin Marietta Corp., 1989.
- 13 Brauer, G. L., Cornick, D. E., Olson, D. W., Peterson, F. M., and Stevenson, R., *Program to Optimize Simulated Trajectories (POST)*, Vol. II, Martin Marietta Corp., 1989.

- 14 Vinh, N. X., *Optimal Trajectories in Atmospheric Flight*, Elsevier Scientific Publishing Co., Amsterdam, 1981.
- 15 Seywald, H., "A Finite Difference Based Method for Automatic Costate Estimation", AIAA Guidance, Navigation, and Control Conference Proceedings, Scottsdale AZ, pp. 368-379, Aug. 1994



## INITIAL DISTRIBUTION LIST

	Number of Copies
1. Defense Technical Information Center 8725 John J. Kingman Rd., STE 0944 Ft. Belvoir, Virginia 22060-6218	2
2. Library, Code 052 Naval Postgraduate School Monterey, California 93943-5101	2
3. Department Chairman, Code AA Department of Aeronautics and Astronautics Naval Postgraduate School Monterey, California 93943-5000	1
4. Department of Aeronautics and Astronautics ATTN: Professor I. M. Ross, Code AA/Ro Naval Postgraduate School Monterey, California 93943-5000	10
5. Space Systems Academic Group ATTN: Lieutenant Commander William Clifton, Code SP/CW Naval Postgraduate School Monterey, California 93943-5000	1
6. Space Warfare Center/DO ATTN: Deputy Director 720 Irwin Ave. (Stop 82-02) Falcon Air Force Base Colorado Springs, Colorado 80912-7210	1
7. Space Warfare Center/IN ATTN: Deputy Director 720 Irwin Ave. (Stop 82-02) Falcon Air Force Base Colorado Springs, Colorado 80912-7210	1
8. Space Warfare Center/AE ATTN: Deputy Director 720 Irwin Ave. (Stop 82-02) Falcon Air Force Base Colorado Springs, Colorado 80912-7210	1

9. Space Warfare Center/XR  
ATTN: Deputy Director  
720 Irwin Ave. (Stop 82-02)  
Falcon Air Force Base  
Colorado Springs, Colorado 80912-7210

1